

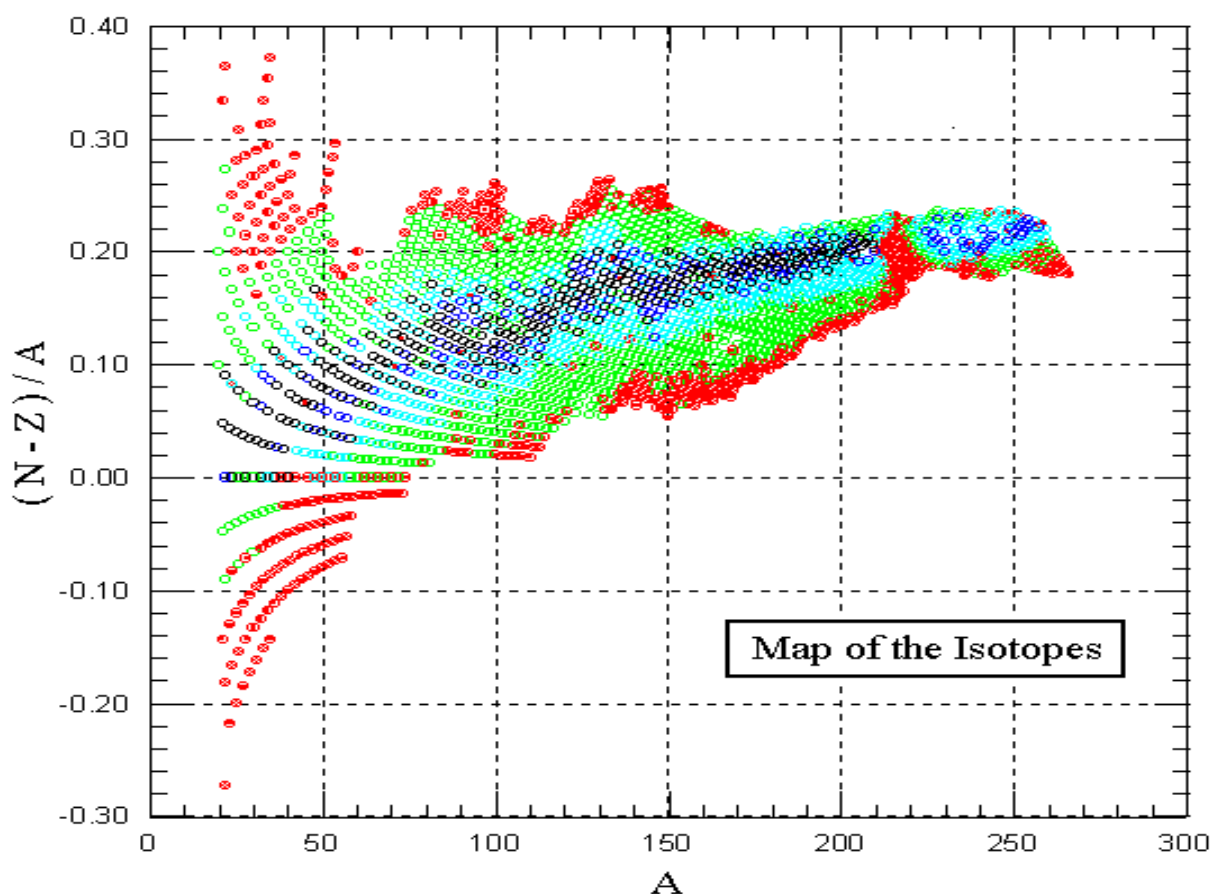
NUCLEAR DATA AND MEASUREMENT SERIES

ANL/NDM-154

An Approach for Dealing with Large Errors

Donald L. Smith, Dmitri G. Naberejnev, and Laura A. Van Wormer

September 2001



ARGONNE NATIONAL LABORATORY
9700 SOUTH CASS AVENUE
ARGONNE, ILLINOIS 60439, U.S.A.

Operated by THE UNIVERSITY OF CHICAGO for the U.S.
DEPARTMENT OF ENERGY under Contract W-31-109-Eng-38

Argonne National Laboratory, with facilities in the states of Illinois and Idaho, is owned by the United States Government, and operated by The University of Chicago under the provisions of a contract with the Department of Energy.

----- **DISCLAIMER** -----

This report was prepared as an account of work sponsored by an agency of the United States Government. Neither the United States Government nor any agency thereof, nor The University of Chicago, nor any of their employees or officers, makes any warranty, express or implied, or assumes any legal liability or responsibility for the accuracy, completeness, or usefulness of any information, apparatus, product, or process disclosed, or represents that its use would not infringe privately owned rights. Reference herein to any specific commercial product, process, or service by trade name, trademark, manufacturer, or otherwise, does not necessarily constitute or imply its endorsement, recommendation, or favoring by the United States Government or any agency thereof. The views and opinions of document authors expressed herein do not necessarily state or reflect those of the United States Government or any agency thereof, Argonne National Laboratory, or The University of Chicago.

Available for a processing fee to U.S. Department of Energy and its contractors, in paper, from:

U.S. Department of Energy
Office of Scientific and Technical Information
P.O. Box 62
Oak Ridge, TN 37831-0062
Internet: <http://www.osti.gov/>
Phone: +1(865)576-1188 (OSTI general information)
+1(865)576-8401 (document ordering service)
Fax: +1(865)576-5728
E-mail: reports@adonis.osti.gov

ANL/NDM-154

An Approach for Dealing with Large Errors ^a

Donald L. Smith ^b and **Dmitri G. Naberejnev**

Technology Development Division
Argonne National Laboratory
9700 South Cass Avenue
Argonne, Illinois 60439
U.S.A.

and

Laura A. Van Wormer ^c

Department of Physics
Hiram College
Hiram, Ohio 44234
U.S.A.

September 2001

Keywords

DATA ANALYSIS. Errors. Uncertainty. Probability. Non-linearity. Radioactivity.
Shielding, Astrophysics.

^a This work was supported by the U.S. Department of Energy, Office of Science, Office of High Energy and Nuclear Physics, Division of Nuclear Physics (SC-23) under Contract W-31-109-Eng-38.

^b Corresponding author – Tel: +1(630)252-6021; Fax: +1(630)252-5287; E-mail: Donald.L.Smith@anl.gov.

^c Summer Research Associate supported by Office of Science, Office of High Energy and Nuclear Physics, Division of Nuclear Physics (SC-23) under Grant DE-FG02-99ER41116.

Nuclear Data and Measurement Series

The Nuclear Data and Measurement Series presents results of studies in the field of microscopic nuclear data. The primary objective is the dissemination of information in the comprehensive form required for nuclear technology applications. This Series is devoted to: a) measured microscopic nuclear parameters, b) experimental techniques and facilities employed in measurements, c) the analysis, correlation and interpretation of nuclear data, and d) the compilation and evaluation of nuclear data. Contributions to this Series are reviewed to assure technical competence and, unless otherwise stated, the contents can be formally referenced. This Series does not supplant formal journal publication, but it does provide the more extensive information required for technological applications (*e.g.*, tabulated numerical data) in a timely manner.

Table of Contents

Information About Other Issues of the ANL/NDM Series	7
Abstract	9
1. Introduction	11
2. Principle of Maximum Entropy and Specification of Probability Distributions	15
3. Non-linear Functions and the Error-amplification Effect	19
4. Deterministic Calculations and Error Propagation	21
5. Monte Carlo Simulation	23
6. Normal Probability Distribution	27
7. Lognormal Probability Distribution	29
8. Some Practical Considerations	31
9. Application to Radioactive Decay	33
10. Application to Radiation Shielding	35
11. Application to Astrophysical Nuclear Reaction Rates	39
12. A Final Look at Errors and the Effects of Non-linearity	47
13. Concluding Remarks	49
Acknowledgements	51
References	53
Tables	57
Figures	67

(Blank Page)

Information About Other Issues of the ANL/NDM Series

Information about all other reports in this Series is available from Argonne National Laboratory via the Internet at the following URL:

<http://www.td.anl.gov/reports/ANLNDMReports.html>

There, one can also find a list of titles and authors, abstracts and specific reports available for viewing or downloading as PDF files.

If any questions arise concerning the present report, the above-mentioned Internet site, or other reports in the Series, please direct them to:

Dr. Donald L. Smith or Dr. Filip G. Kondev
Nuclear Data Program
Technology Development Division
Building 362
Argonne National Laboratory
9700 South Cass Avenue
Argonne, Illinois 60439
U.S.A.

Tel: +1(630)252-6021 (Donald L. Smith)
+1(630)252-4484 (Filip G. Kondev)
Fax: +1(630)252-5287
E-mail: Donald.L.Smith@anl.gov
Kondev@anl.gov

(Blank Page)

An Approach for Dealing with Large Errors ^a

by

Donald L. Smith ^b and **Dimitri G. Naberejnev**

Technology Development Division, Argonne National Laboratory
Argonne, Illinois 60439, U.S.A.

And

Laura A. Van Wormer ^c

Department of Physics, Hiram College
Hiram, Ohio 44234, U.S.A.

ABSTRACT

Numerical functions or equivalent algorithms are commonly used to derive estimates for physical quantities that can be expressed in terms of more fundamental physical parameters. It is shown that in situations where large uncertainties (errors) are involved in these parameters, or where error amplification occurs through severe non-linearity of the functions, conventional deterministic techniques for calculating the derived quantities and estimating their errors can lead to erroneous results. Instead, it is necessary to resort to a probabilistic approach and thereby obtain estimates for mean values and variances of the derived quantities through Monte Carlo simulation in order to preserve the essential information without distortion. The correct choice for a probability distribution is suggested by the inherent nature of the random variable in question. Examples are given from the analysis of radioactivity decay, the shielding of penetrating radiation, and the derivation of nuclear reaction rates that are used in astrophysical calculations to model nucleosynthesis of the elements in stellar explosions. Subsequent analyses that use these derived quantities must also be carried out in a probabilistic manner to insure that the obtained results will reflect the underlying information properly.

^a This work was supported by the U.S. Department of Energy, Office of Science, Office of High Energy and Nuclear Physics, Division of Nuclear Physics (SC-23) under Contract W-31-109-Eng-38.

^b Corresponding author – Tel: +1(630)252-6021; Fax: +1(630)252-5287; E-mail: Donald.L.Smith@anl.gov.

^c Summer Research Associate supported by Office of Science, Office of High Energy and Nuclear Physics, Division of Nuclear Physics (SC-23) under Grant DE-FG02-99ER41116.

(Blank Page)

1. Introduction

In basic and applied science, as well as in engineering applications, there is frequent need to consider a physical quantity or a set of physical quantities that can, in turn, be derived from one or more fundamental parameters. It is a well-established theorem of statistics that a quantity that is related to a random variable through a well-defined and well-behaved (continuously differentiable) functional relationship can also be treated as a random variable and therefore possesses its own associated probability distribution [1]. To illustrate this point, let us suppose that

$$y = f(x). \quad (1)$$

Here, x is a single, primary random variable governed by the normalized probability density function p , *i.e.*, a function for which

$$\int p(x)dx = 1. \quad (2)$$

The range of integration extends continuously over all values for which parameter x is defined. In applications, it is typical to assume that if x_a is a particular value of x then $y_a = f(x_a)$ is the appropriate choice for the derived value of y . This deterministic approach can be generalized to treat sets of primary parameters \mathbf{x} and derived quantities \mathbf{y} with arbitrary (finite) dimensionalities, as expressed through the vector functional relationship

$$\mathbf{y} = \mathbf{f}(\mathbf{x}). \quad (3)$$

We will demonstrate that this traditional approach is often inadequate to handle situations where x is so uncertain (large error) that a correspondingly large error results for y . We may also encounter equivalent difficulties if the function f is non-linear, possibly leading to severe conditions that can produce error amplification. Then, the error in y might be quite large even when the error in x is relatively small. The same comments can be applied to sets of primary random variables and their functional relationships, but for convenience we will restrict the present discussion to a single variable and function.

There is no need to define “non-linearity” in the context of a function f . This particular concept is quite unambiguous. What does require definition here are the expressions “large error” and “severe condition”.

For present purposes we will define an error in x to be “large” if x is governed by a probability distribution function p that possesses a well defined mean value

$$m_x = \langle x \rangle = \int x p(x)dx, \quad (4)$$

yet at the same time this probability function is observed to be quite broad in shape and often asymmetrically distributed with respect to its mean value [1]. Expressed more precisely, the variance

$$\mu_{2x} = \langle (x - m_x)^2 \rangle = \int (x - m_x)^2 p(x) dx \quad (5)$$

and the corresponding standard deviation

$$s_x = (\mu_{2x})^{1/2} \quad (6)$$

that are associated with the probability function p are significantly large. For practical considerations, it turns out that in this context the borderline between “small” and “large” errors (standard deviations) corresponds to fractional errors on the order of 30%. The reason for this particular boundary point selection is that the applicable probability distribution, as we shall see more clearly from the discussion in Section 7 and Fig. 4, become noticeably skewed for an error that is larger than this value.

A “severe” condition is said to exist when

$$m_y \equiv \langle y \rangle \neq f(m_x) \quad (7)$$

and, furthermore, m_y differs significantly from $f(m_x)$. In other words, when the inequality expressed in Eq. (7) is considerable. For the formulas considered in this report, we choose to use the notation $\langle \dots \rangle$ to signify averages of random variables with respect to the applicable probability distribution functions. What is a “significant” difference? There is no rigorous answer to this question. From a practical point of view, a difference becomes significant when the bias introduced by assuming that $\langle y \rangle = f(m_x)$ leads to a systematic deviation (systematic error or bias) in the derived physical quantity that is unacceptable to the user in a particular application. It is important to realize that such a bias will develop to some extent in all non-linear functional relationships, and that it need not be a consequence of a breakdown in applicability of the mathematical formulation of the physical problem. In fact, many features of the physical world can be modeled only by using non-linear functions. Often, these small differences are neglected, but we will be examining cases in this report where they cannot be ignored. While random error tends to be unavoidable, and possibly dominant, scientists should resort to whatever means possible to minimize the effects of systematic error.

The main objective of this paper is to demonstrate an approach that allows physical problems involving very large errors and severe conditions to be handled with minimal loss of the fundamental information content inherent to these problems. By “fundamental information” it is meant, in this context, detailed knowledge of the probability distribution(s) which govern the observation (measurement) process by which we gain information about the physical phenomena that interest us. Consequently, the method that will be discussed in this paper involves consideration of the underlying probability function(s) for the random variable(s) as well as the development of a consistent way to parameterize the essential information content efficiently without jeopardizing its fidelity. In short, we will suggest an approach to data compression that nevertheless optimizes both fidelity and preservation of critical information. This topic is of considerable practical interest because large errors and severe conditions arise in a

variety of realistic physical problems. Three of these situations are examined in the present paper to illustrate the concepts. Those processes to be considered are radioactive decay over long time periods, deep-penetration radiation shielding, and the determination of astrophysical nuclear reaction rates at low stellar temperatures. Finally, we shall take another look at some effects of errors and non-linearity.

(Blank Page)

2. Principle of Maximum Entropy and Specification of Probability Distributions

It is apparent from the discussion in Section 1 that knowledge of the probability density function p is essential in situations where large errors have to be considered. How should it be determined? It is commonly assumed that the normal (Gaussian) probability function is the appropriate one to use. If more than one variable is involved, then the multi-variate normal distribution is often applied. We shall see that this assumption may have to be abandoned in certain situations where the errors are large and the conditions severe. In order to obtain guidance concerning the appropriate selection of a probability function, it is necessary to invoke the Principle of Maximum Entropy [1,2,3] which is one of the foundations of modern Information Theory [4]. This theoretical recipe tells us that the best choice of a probability function p is established unambiguously once we specify the basic properties of the random variable in question. For example, if we assume that the variable x can take on any value between $-\infty$ and $+\infty$, and we possess only an estimate of the mean value m_x and its standard deviation s_x , then the optimal choice for p is indeed the normal probability function. However, since most physical parameters, such as cross sections, particle kinetic energies, resonance strengths, *etc.*, are represented by inherently positive numbers, *i.e.*, $x > 0$, the normal probability distribution may not be appropriate in extreme situations since it does not prevent x from occasionally becoming negative. We shall demonstrate this point in Section 6. If $x > 0$ and we possess only estimates for m_x and s_x , we should employ the lognormal distribution for p [3]. If we know only that $x > 0$, but have no other knowledge about this random variable, then we ought to apply Jeffreys' Prior distribution [5]. This rule dictates that the probability function for $\ln x$ be uniformly distributed from $-\infty$ and $+\infty$ or, equivalently, that

$$p(x) \propto 1/x \quad (\text{for } x > 0). \quad (8)$$

If we know that x lies somewhere in the range (x_{\min}, x_{\max}) , but have no additional information concerning p , then a modified version of Jeffreys' Prior distribution is appropriate. It should then be assumed that $\ln x$ is uniformly distributed over the range $(\ln x_{\min}, \ln x_{\max})$ and that there is zero probability of x being found outside this range. We will learn more about the important normal and lognormal probability distributions and their relationships to each other in Sections 6 and 7.

Regardless of which probability function is applicable to a particular situation, it is those specific parameters that characterize this function which contain all of the essential information content [1]. These parameters are generally closely related to low-order moments of the probability function. In particular, the mean value and standard deviation are generally considered to be the most crucial of these moments. Therefore, we should always interpret the "value" and "error" of a particular physical quantity (measured or evaluated) as being the "mean value" and "standard deviation", respectively, corresponding to the applicable probability distribution function. In the presence of uncertainty, no other interpretation is consistent with reality. This probability function governs the outcome of any sampling process (actual measurements or simulated using Monte Carlo techniques) associated with the random variable that

represents the physical quantity in question. This specific probability function will belong to a particular category of functions according to the actual knowledge we have about the physical quantity under consideration. In many cases the functional category itself will belong to the broad family of functions known as gamma functions [3].

Finally, we will examine very briefly in this section how information derived from a functional relationship, as described above, should be interpreted in the presence of large errors. We have already noted in Section 1 that assuming a deterministic relationship between a primary physical parameter x and a derived one y may lead to biased results. If a functional relationship f exists between random variables x and y , as indicated in Eq. (1) – and x has a large error with (very likely) an associated asymmetric probability density function p – it will be necessary to deal with the resulting probability density function q corresponding to y rather than considering just one specific value of y . In some cases this probability function q can be derived by analytical transformation from p , but more often than not it will be necessary to generate an approximation to q empirically through random sampling (*i.e.*, by using the Monte Carlo method) [1]. If the functional relationship between x and y is known, it is a straightforward exercise to obtain estimates for the mean value m_y and standard deviation s_y of the probability distribution q for the derived variable y – without having knowledge of the detailed nature of q – by using a sampling procedure. The applicable formulas are

$$m_y \approx \langle y \rangle \tag{9}$$

and

$$s_y \approx [\langle y^2 \rangle - m_y^2]^{1/2}, \tag{10}$$

where the indicated averages $\langle \dots \rangle$ are calculated in the usual Monte Carlo fashion from the accumulated collection of sample values $y_1 = f(x_1)$, $y_2 = f(x_2)$, \dots , $y_N = f(x_N)$ resulting from a sampling sequence that produced x_1 , x_2 , \dots , x_N . Here, N denotes the number of traced sampling “histories” [1]. Approximate equality is indicated in Eqs. (9) and (10) because results obtained from Monte Carlo sampling are never exact, no matter how many histories N are traced. When we have no other basis for selecting a particular probability distribution function q other than empirical results from sampling, there is a convenient option available. For pragmatic reasons we may decide not to deal with the empirical distribution that results from sampling (with all of its numerical detail). We could instead simply choose to invoke the Principle of Maximum Entropy and accept the particular probability distribution type that is dictated by the information we intend to retain from the sampling exercise. However, in so doing we should be aware that we deliberately are choosing to reject some potentially useful knowledge about the derived variable y . It would be unfortunate to do this after having already performed an extensive set of Monte Carlo simulation calculations. We really need to be sure of how the retained information is to be used in subsequent applications before deciding what information to retain and what to discard. We also should be cognizant of the fact that a decision to reject information could lead to a violation of certain fundamental rules of statistics.

These decisions obviously call for the exercise of good judgement rather than blind reliance on mathematical algorithms.

(Blank Page)

3. Non-linear Functions and the Error-amplification Effect

A linear function of a single random variable can be expressed in the form

$$y = f(x) = a_0 + a_1 x \quad (11)$$

where a_0 and a_1 signify ordinary constants. For simplicity, we shall assume that a_0 , a_1 , and x are positive numbers. Simple error propagation analysis utilizes the formula

$$s_y \approx |df/dx| s_x = a_1 s_x, \quad (12)$$

where the notation $|\dots|$ means absolute value and “s” denotes standard deviation. The fractional error in y can then be determined in terms of the fractional error in x . We obtain the following result:

$$s_y/y \approx a_1 s_x / (a_0 + a_1 x) = [a_1 x / (a_0 + a_1 x)] (s_x/x) < s_x/x. \quad (13)$$

There is no error amplification since the fractional (or percent) error in y cannot exceed the corresponding error in x for this situation.

The same cannot be said for non-linear functions. Before generalizing, we offer two specific examples that serve to illustrate the point. Suppose, *e.g.*, that

$$y = f(x) = x^3 \quad (x > 0). \quad (14)$$

It can be shown easily by a similar analysis that

$$s_y/y \approx 3 s_x/x. \quad (15)$$

This corresponds to a fixed error-amplification factor of 3 regardless of x . Another interesting example that has important practical implications involves the exponential function. Suppose that

$$y = f(x) = a_0 \exp(a_1 x) \quad (x > 0), \quad (16)$$

where a_0 and a_1 are both positive. Following the same procedure we find that

$$s_y/y \approx (a_1 x) s_x/x. \quad (17)$$

The error-amplification factor “ $a_1 x$ ” depends upon x and it can be exceedingly large if x is very large. Of course this elementary approach to error estimation is overly simplistic, and it tends to break down when the errors involved become large. It is based on considering only the first-order terms of a Taylor’s series [1]. Nevertheless, these simple examples do illustrate the inherent difficulties that may be encountered in dealing with large errors and non-linear functions, even when the more rigorous probabilistic

approach considered in the present investigation is pursued. In any event, it is evident from an examination of Eqs. (11), (12), (15), and (17) that extreme conditions arise in a single variable case when $\{(x/y) |df/dx|\} \gg 1$.

4. Deterministic Calculations and Error Propagation

The deterministic approach to calculating derived quantities and their errors – as embodied in Eqs. (1) and (12) and easily extended for multiple variables to include derivation of covariance information (errors and correlations) by the application of a first-order Taylor’s series approximation – is widely used in basic and applied science [1]. It is also the starting point for data-fitting exercises based on applications of the least-squares method [1,6]. This approach will be employed in the present investigation to provide deterministic values that can be compared with results obtained from a more general probabilistic approach to the specification of derived values and their errors. Since the probabilistic approach is sometimes awkward to apply – and is certainly demanding of computing resources in many instances – the deterministic approach should be used wherever it provides sufficiently accurate results. Normally, this will be the case when errors are relatively small and the conditions not extreme. In this section, we offer a brief review of the deterministic approach. As mentioned above, we begin with Eqs. (1) and (12). In particular, we consider a collection of primary random variables \mathbf{x} and a set of functions \mathbf{f} that lead to derived variables \mathbf{y} . These sets have finite dimensions. For a particular \mathbf{x}_a , we assume from Eq. (3) that

$$\mathbf{y}_a \approx \mathbf{f}(\mathbf{x}_a) . \quad (18)$$

The covariance matrix for \mathbf{y} , corresponding to that specific \mathbf{y}_a , is obtained from the matrix formula

$$\mathbf{V}_y \approx \mathbf{T}^+ \mathbf{V}_x \mathbf{T} . \quad (19)$$

The elements t_{ik} of matrix \mathbf{T} are given by the expression

$$t_{ik} = (\partial f_i / \partial x_k)_a . \quad (20)$$

The subscript “a” indicates that these matrix elements are calculated using $\mathbf{x} = \mathbf{x}_a$. We have indicated approximate equality in Eqs. (18) and (19) to remind ourselves of the underlying approximations involved in deriving these formulas and of our interpretation of “value” as “mean value” and “error” as “standard deviation”. The square roots of the diagonal elements of \mathbf{V}_x and \mathbf{V}_y correspond to errors in the various components of \mathbf{x} and \mathbf{y} , respectively. The off-diagonal elements provide information on the assumed (in the case of \mathbf{x}) or derived (in the case of \mathbf{y}) correlation parameters for these errors. This approach is popular because it is straightforward and not computationally intensive. Unfortunately, this approach can lead to incorrect results when the errors become large and the conditions severe.

(Blank Page)

5. Monte Carlo Simulation

In this section we describe a probabilistic approach that yields results which are comparable to those provided by the deterministic method discussed in Section 4 whenever one is dealing with modest errors. However, it is technically more appropriate for handling cases involving large errors. This Monte Carlo simulation method generates a discrete approximation to the “true” continuous, joint probability density function q for a set of derived random variables \mathbf{y} . The discrete representation of q is obtained by allocating numerical values obtained from sampling outcomes to pre-defined numerical intervals that span pre-determined, inclusive ranges of values for the derived random variables. A tally is kept of the outcomes from all the sampling histories. In this manner, the appropriate joint probability function q corresponding to a set of derived variables \mathbf{y} is estimated empirically from given probability information p about the primary variables \mathbf{x} and a set of functions \mathbf{f} that relate these two sets of variables.

This procedure involves a relatively straightforward extension of the formalism described for single variables as embodied in Eqs. (9) and (10). A collection of primary random vectors $\mathbf{x}_1, \mathbf{x}_2, \dots, \mathbf{x}_N$ is generated by Monte Carlo sampling. The sampling takes place within pre-defined, inclusive primary parameter ranges in accordance with the applicable probability distribution for these variables. If error correlations exist between the components of these vectors, *i.e.*, if \mathbf{V}_x is not diagonal, then care must be taken to assure that existing non-zero correlations are reflected in the sampling procedure. However, in those specific cases that we have studied during the present investigation it was assumed, for convenience, that such correlations do not exist and, therefore, that each component x_i of the vector \mathbf{x} is governed by an independent probability distribution p_i . Thus, for this special situation

$$p(\mathbf{x}) = \prod_i p_i(x_i) . \quad (21)$$

A collection of derived vectors $\mathbf{y}_1 = \mathbf{f}(\mathbf{x}_1), \mathbf{y}_2 = \mathbf{f}(\mathbf{x}_2), \dots, \mathbf{y}_N = \mathbf{f}(\mathbf{x}_N)$ is generated by this sampling procedure. Depending upon how the Monte Carlo computer program is written, one can choose to retain all or simply a portion of the resulting information about \mathbf{y} generated by this approach. For the purpose of this discussion, “all” implies a detailed representation of the probability distribution q for \mathbf{y} whereas “a portion” suggests information about just a few selected moments of this function [1]. For example, Eqs. (9) and (10) can be generalized to yield the following expressions for the important low-order moments of q , namely,

$$m_{y_i} \approx \langle y_i \rangle \quad (22)$$

and

$$(\mathbf{V}_y)_{ij} \approx \langle y_i y_j \rangle - m_{y_i} m_{y_j} , \quad (23)$$

where $(\mathbf{V}_y)_{ij}$ is an element of covariance matrix \mathbf{V}_y . The standard deviations are defined by the formula

$$s_{yi} = [(\mathbf{V}_y)_{ii}]^{1/2}. \quad (24)$$

When there are multiple derived quantities \mathbf{y} , a covariance matrix with (very likely) non-zero off-diagonal elements will be generated regardless of whether or not non-zero error correlations are assumed for the primary variables \mathbf{x} . This outcome is very similar qualitatively to what emerges from an application of the deterministic approach discussed in Section 4.

The knowledge gap that exists between possessing information about a few low-order moments of a probability function and having complete knowledge of the probability function itself may disappear if it is understood to which family of functions that distribution ought to belong – based on fundamental considerations or empirical observations. Many well-known, useful probability distributions, including the normal (Gaussian) and lognormal functions discussed in Sections 6 and 7, respectively, are uniquely characterized by their low-order moments. The implications of this fact are crucial to the present investigation; they will be discussed in later sections of this paper.

Next, we address the following question: How many Monte Carlo sampling histories N should be followed – and what range(s) of primary random variable space(s) need to be sampled – in order to generate reliable estimates for the moments of the probability distribution q that are applicable to the derived random variable(s) and/or to determine the more detailed shape of q itself? The specific answer to this question depends intimately on the nature of the random variables x and y (or \mathbf{x} and \mathbf{y} for the multivariate situation). However, there is a simple principle that can offer some guidance: The sampling range(s) and number of Monte Carlo histories that should be considered in a particular calculation are intimately related. For simplicity, we shall consider the case of a single, primary random variable x with probability distribution p . This function is assumed to have a well-defined mean value m_x and standard deviation s_x , as discussed above. We shall suppose also that the sampling range is the interval (x_{\min}, x_{\max}) . Naturally, $x = m_x$ should fall within this range. Let η be a positive “range” constant such that the conditions $(m_x - x_{\min}) \leq \eta s_x$ and $(x_{\max} - m_x) \leq \eta s_x$ are both satisfied. Then, we can ask the following well-defined question: Given η , what is the minimum number of sampling histories N required in order to insure that this random-variable interval is adequately sampled? In those situations where the probability distribution p is reasonably well localized and tends to be “peaked” in shape either near the mean value or the mode of the distribution (the mode x_0 is defined by the condition $p(x) \leq p(x_0)$ for all x in the sampling range), a very rough guideline is provided by considering the expression

$$p(m_x \pm \eta s_x)/p(m_x) < N^{-1}. \quad (25)$$

The reader should be aware that this formula has no rigorous mathematical justification, but rather it is based on the experience gained from performing such calculations, including the many exercises carried out during the present investigation. This formula

evolved from the notion that when a limited number of Monte Carlo histories are followed, the odds of encountering values of a particular random variable that are far removed from the mean value (as measured in units of standard deviation) are very small. Consequently, there is nothing materially gained by attempting to sample values in this region of parameter space. By invoking this criterion, one can improve the sampling efficiency of a Monte Carlo exercise. By the same token, this formula can also be employed to suggest a reasonable choice for η when, for practical reasons, one is limited to a particular value of N . For example, if p is a univariate normal probability distribution – that is symmetric about the mean value and reasonably well localized – we can deduce quite easily the following suggested sampling-condition relationships by an application of Eq. (25): $\eta = 1.0 \Leftrightarrow N > 2$; $\eta = 2.0 \Leftrightarrow N > 7$; $\eta = 3.0 \Leftrightarrow N > 90$; $\eta = 4.0 \Leftrightarrow N > 2981$; $\eta = 5.0 \Leftrightarrow N > 268337$; $\eta = 6.0 \Leftrightarrow N > 65659969$. Clearly, Eq. (25) is not very useful for small values of η . However, for $\eta > 3.0 - 4.0$, it can be a valuable tool in practical exercises of the Monte Carlo Method. There are other considerations that may lead to refinement of the process of selecting a sampling range and number of histories to utilize in Monte Carlo simulations. Statistical accuracy of the desired results is certainly an important factor. Another technical consideration is the fidelity (true randomness) of the random-number generator employed for Monte Carlo sampling [1]. For those specific cases that are discussed in later sections of this paper, extensive studies were carried out concerning the convergence behavior for various choices of η and N . Most of the calculations performed during the course of the present investigation employed $N = 10^6$ and $\eta = 5.0$ as a compromise between desired accuracy and computer time required for the Monte Carlo simulations. A large number of calculations were also performed using $N = 9 \times 10^6$ and $\eta = 8.0$ to see if significant differences in outcomes would develop. A few of the simulation exercises involved even more histories and wider parameter sampling ranges. In all these latter cases, we found no justification for employing such large numbers of Monte Carlo sampling histories or sampling ranges this broad in the simulations performed during this investigation.

(Blank Page)

6. Normal Probability Distribution

For simplicity, we will discuss the univariate case. The Central Limit Theorem tells us that whenever a particular physical quantity is subjected to a large number of small, unrelated additive (+ or -) disturbances, then the limiting probability distribution is normal [1]. For a single random variable x , the probability density function, *i.e.*, the function that must be integrated to obtain true probability, takes the normalized form

$$p(x) = (2\pi\mu_{2x})^{-1/2} \exp [-(x - m_x)^2/2\mu_{2x}] \quad (-\infty < x < +\infty), \quad (26)$$

where mean value m_x and variance μ_{2x} are defined by Eqs. (4) and (5). Furthermore, in Section 2 it was pointed out that the Principle of Maximum Entropy suggests that if a random variable x can assume any value between $-\infty$ and $+\infty$, and all that we know about its probability distribution p are estimated values for the mean value and standard deviation (error), then our best assumption is that p should be a normal distribution [1,2,3]. These two arguments – along with the fact that the Gaussian function has some convenient features – have led many scientists to assume that most experimentally determined physical quantities can be described by normally distributed random variables.

Is the normal probability function appropriate for the description of real, positive physical quantities under extreme conditions, *e.g.*, when there are large errors? We will examine the behavior of the normal probability distribution with the specific intent of showing that there exist circumstances where its use can lead to serious difficulties in dealing with inherently positive random variables. The fact that there is a non-negligible possibility of selecting negative values when performing Monte Carlo sampling exercises involving the normal distribution – even when the mean value is positive – has been pointed out recently by Hix *et al.* [7]. As an example, we suppose that $m_x = 100$. Fig. 1 compares the probability distribution shapes for standard deviations $s_x = 1, 10, 20, 50, 100,$ and 150 , respectively. This figure demonstrates that there is little possibility of encountering a negative value for $s_x \leq 20$. However, for $s_x \geq 30$ (an error of 30% or larger), a significant chance develops of encountering a non-physical result in Monte Carlo sampling when using a Gaussian function. This point is made clear quantitatively in Fig. 2. It is seen that for the case of 100% error, the chance of obtaining a negative value of x in sampling is $> 15\%$. For 150% error, over 25% of the sampled values x are expected to be negative. So, as anticipated, we must conclude that the normal distribution is inadequate to deal with inherently positive physical quantities that involve very large errors. A new approach must be sought to circumvent this problem. However, it is essential that – in the limiting case of relatively small errors – the “correct” probability function should behave very similarly to the normal distribution and yield comparable results in sampling exercises.

(Blank Page)

7. Lognormal Probability Distribution

A possible solution to the “negative-value” problem mentioned in Section 6 is to employ the lognormal function for probabilistic analyses involving inherently positive random variables and severe conditions [1]. For a single random variable, this distribution takes the normalized form

$$p(x) = (2\pi\sigma^2x^2)^{-1/2} \exp[-(\ln x - v)^2/2\sigma^2] \quad (x > 0). \quad (27)$$

The mean value and standard deviation are obtained by using the formulas

$$m_x = \exp[v + (\sigma^2/2)] \quad (28)$$

and

$$\mu_{2x} = s_x^2 = m_x^2 [\exp(\sigma^2) - 1] = \exp(2v + 2\sigma^2) - \exp(2v + \sigma^2). \quad (29)$$

Conversely, if the mean value m_x and variance μ_{2x} for this distribution are given, then those parameters v and σ that characterize the lognormal function can be derived from the expressions

$$\sigma^2 = \ln [1 + (\mu_{2x}/m_x^2)] \quad (30)$$

and

$$v = \ln m_x - (\sigma^2/2). \quad (31)$$

When the probability function for x is assumed to be lognormal, then the distribution for $y = \ln x$ is normal [1]. The converse is also true. In this sense, these two functions are conjugates of each other. This fact has been exploited extensively in the present investigation.

The lognormal function clearly exhibits the desired property of non-negativity over the variable range for which it is defined ($x > 0$), no matter how large a standard deviation is involved. However, we must explore the issue of whether this probability distribution selection can be justified on more fundamental grounds. It can be shown that the lognormal probability function is the limiting distribution for an inherently positive random variable subjected to many positive multiplicative disturbances that vary only slightly from unity [3]. There is an obvious analogy here to the conditions that generate the normal distribution, as discussed in Section 6. In fact, a multiplicative disturbance to a positive random variable x is completely equivalent to an additive disturbance to $\ln x$ [7]. Furthermore, as was mentioned in Section 2, the Principle of Maximum Entropy [1,2,3] tells us that the optimal choice of a probability distribution for an inherently positive random variable is the lognormal function when one possesses specific knowledge only of the mean value and standard deviation. The lognormal function differs

from the normal (Gaussian) function in that its shape is not symmetric about the mean value. In fact, the lognormal probability function is inherently asymmetric and attains its maximum value at the mode x_0 given by the formula

$$x_0 = \exp(\nu - \sigma^2). \quad (32)$$

Due to the asymmetric nature of the lognormal distribution mentioned above, the mode x_0 always differs from the mean value m_x . This difference will be very small when the standard deviation is small relative to the mean value. Under these conditions, the normal and lognormal distributions have very similar shapes. For example, let us suppose that $m_x = 100$. Fig. 3 compares the probability distribution shapes for standard deviations $s_x = 1, 10, 20, 50, 100,$ and 150 , respectively. For small standard deviations, the shape of the lognormal distribution appears to be reasonably symmetric and is rather similar to that of a normal distribution. However, as s_x increases the lognormal distribution clearly exhibits its decidedly asymmetric nature. For extremely large standard deviations, the lognormal function actually approaches Jeffrey's Prior distribution, as defined in Eq. (8), except for the very smallest values of x [5]. This is consistent with the intuitive notion that if the uncertainty is extremely large we obviously possess very little information about the random variable in question.

Finally, it is interesting to compare directly the shapes of normal and lognormal distributions with equivalent mean values and standard deviations. A few examples are shown in Fig. 4. There it is assumed that $m_x = 100$ and $s_x = 20, 50, 100,$ and 150 , respectively, for both probability functions. In each of these plots, the two functions are normalized so that their integral values $\int p(x)dx$ are equal.

8. Some Practical Considerations

The preceding sections of this paper offer several qualitative mathematical arguments for selecting the lognormal distribution function to represent inherently positive physical quantities. The discussion concerning this distribution that appears in Ref. [1] mentions that it has been shown definitively to apply to such diverse situations as the analysis of incomes, the distribution of classroom sizes, and the observed masses or sizes of biological organisms. A feature that these diverse examples share is the inherent positive nature of the observable variables. While this accumulated evidence does not prove rigorously that the lognormal distribution should be applied to positive variables in all instances, it certainly appears to be a very reasonable assumption from a pragmatic point of view. Therefore, we shall assume, for present purposes, that an inherently positive primary random variable x is indeed distributed according to a lognormal function p , provided that our information about that variable is limited to knowledge of the distribution mean value and standard deviation. By “primary” we mean a random variable that represents a directly measured physical quantity.

To pursue this matter further, we pose the following two questions: 1) If $x > 0$ is accepted *a priori* to be distributed according to a lognormal probability function p , and y and x are related through a well-defined, continuous and differentiable function f , according to Eq. (1), in such a manner that $y > 0$, should we expect the probability distribution q for y to be lognormal? 2) If so, could this result be generalized to include situations involving multiple variables? Since the statistical nature of x is specified, along with knowledge of the function f that links x to y , the probability distribution q for y can certainly be determined directly – if not analytically, then empirically by Monte Carlo simulation. A conservative approach would be to assume that it is unreasonable to expect *a priori* that the true probability distribution q for y should be identical to a lognormal function, or equivalently, that the probability distribution for $\ln y$ should be identical to a normal (Gaussian) function. In the present investigation, we have explored the extent to which the true probability function q for a derived random variable y – as deduced by Monte Carlo simulation – resembles a lognormal function or, equivalently, how well $\ln y$ can be described by a normal distribution. Experience gained from extensive numerical studies we performed during the course of this investigation appears to confirm that q need not be exactly equal to a lognormal function. However, the actual distributions can usually be approximated quite well – for practical purposes – by lognormal functions, provided that the parameters (distribution moments) are determined properly (Sections 9 – 11).

The present investigation relies heavily on Monte Carlo simulation. Therefore, the first step we took in this project was to demonstrate that our selected Monte Carlo simulation procedures would be able to reproduce a particular sampling distribution to a degree of precision limited only by the coarseness of the chosen interval structure and the selected number of sampling histories N . We employed well-known numerical methods that are described in the literature to generate a sequence of random numbers and thereby replicate the selected probability distribution functions [1,8]. Actually, two distinct

random-number-generator algorithms and approaches to probability-distribution replication were implemented in various computer codes used for numerical studies reported in this work. Both of these approaches yielded nearly identical results (within the expected limits of numerical precision) for equivalent problems. Consequently, no distinction between them is noted in the present discussion. Our first test sought to determine if a simple lognormal distribution with mean value $m_x = 10$ and standard deviation $s_x = 5$ (50% error) could be reproduced well by Monte Carlo simulation. This example reflects a relatively moderate rather than a severe error condition. In this exercise, a modest number of histories, namely, $N = 10^5$, were traced. The sampling results were allocated to 30 intervals of equal width in the variable x spanning a range of that variable corresponding to $\eta = 3.0$, as discussed in Section 5: $x_{\min} = 2.168$ to $x_{\max} = 36.898$. The results are shown in Fig. 5. Tallies of events allocated to these intervals from sampling are plotted in the form of a histogram. A smooth curve that represents the actual considered lognormal probability function p – suitably normalized so that $\int p(x)dx = 100000$ – is also plotted in this figure. It is clear that the agreement is excellent. However, further numerical tests of this nature indicated that when the standard deviation is very large a comparison of this sort is much more difficult to carry out for the lognormal function. Its inherent asymmetry – which is manifested in a rapid variation of p with x as x approaches zero – makes it difficult to replicate the shape of this function using a histogram. This can only be done if a very fine interval structure is selected, a large number of Monte Carlo histories are followed, and the computer that is employed for the calculations is capable of providing excellent numerical precision. Our concern with the constraints that these stringent requirements impose led us eventually to pursue a different approach, namely, to validate that a derived quantity y is represented well by a lognormal distribution by instead verifying that $\ln y$ is described well by a normal distribution. We learned that this latter approach avoids many of the numerical difficulties encountered in working with a highly asymmetric lognormal distribution directly. Unambiguous transformations between the parameters of conjugate normal and lognormal probability distributions can be performed using the formulas that appear in Eqs. (28) - (31).

9. Application to Radioactive Decay

For the storage and disposal of radioactive materials – as well as for decontamination purposes – it is important to be able to predict residual radioactivity levels reliably after elapsed times corresponding to many decay half lives. The decay of a single radioactive species is governed by the formula

$$A = A_0 \exp(-\lambda t) , \quad (33)$$

where t is time, λ is the decay constant, A_0 is the activity at time zero, and A is the activity after elapsed time t . The decay constant λ is related to the mean life τ and half life $t_{1/2}$ by the expression

$$\lambda = 1/\tau = (\ln 2) / t_{1/2} . \quad (34)$$

From Eq. (17) and the related discussion in Section 3, it is evident that the error amplification factor at time t in this particular situation can be deduced from the expression

$$s_A / A \approx \lambda t (s_\lambda / \lambda) . \quad (35)$$

Thus, the error amplification factor in this instance is λt .

In this section we will consider – as an example – the decay of the radioisotope ^{53}V by β^- emission. There is uncertainty associated with the various reported values of half life and, therefore, in the decay constant λ for this radio-nuclide. An evaluation by Browne and Firestone suggests 96.6 ± 2.4 seconds (2.5% error) for the half life [9]. A comparable evaluation published by Tuli recommends 96.0 ± 2.4 seconds (2.5% error) [10]. These two results are quite close. However, a recent evaluation by Smith and Fessler – that reflects their new experimental data as well as existing results – suggests a rather different result, namely, 92.4 ± 1.1 seconds (1.2% error) [11]. Although these do not appear to be large differences, the effect of even small differences can be magnified significantly if the elapsed time is large. We have examined the impact of these differences in ascertaining the residual activity at $t = 3600$ seconds (1 hour) using both deterministic calculations and Monte Carlo simulations, as described in Sections 4 and 5, respectively. Two distinct sets of values for λ and its error were considered. The error amplification factors calculated using Eq. (34) and the half-life values given above are in the range 26 to 27.

Deterministic calculations were carried out in the manner described in Section 4. The Monte Carlo simulation analyses followed procedures that are discussed in Section 5. Only the error in λ was considered; no error is assigned to A_0 . Mean values and standard deviations were estimated first for $\ln A$. They were then used to derive corresponding mean values and standard deviations for A under the assumption that the natural logarithm of the residual activity is normally distributed while the residual

activity itself is described by a lognormal function. The requisite transformation formulas are given in Eqs. (28) and (29). In order to test the validity of this approach, discrete representations of the probability functions for the natural logarithms of the residual activities were generated by Monte Carlo simulation. These shapes were then compared to normal distributions applicable to $\ln A$ with mean values and standard deviations equal to results obtained directly from Monte Carlo simulation using Eqs. (9) and (10). The outcome from this analysis is illustrated in Fig. 6 for the case $\lambda = 0.007220$. While the agreement is not perfect – as could be anticipated from the discussion in Section 8 – it is nevertheless remarkably good over a range of nearly three decades for the probability density function. Consequently, it is reasonable, for most practical purposes, to conclude that the probability density function (PDF) for residual activity A can be described quite well by a lognormal probability distribution function.

The numerical results obtained from this analysis are provided in Table 1. It is apparent that the deterministic and Monte Carlo calculations yield noticeably different mean values for the derived quantities under these severe conditions. There are also very significant differences between the residual activities determined by either method using the evaluated half-life value of Browne and Firestone [9] (also supported by Tuli [10]) and that obtained from the data of Smith and Fessler [11]. Two conclusions emerge from this particular analysis: 1) Precise knowledge of radioactive decay constants is essential when accurate determinations of residual radioactivity – following long decay times (many half lives) – are sought. This is often a requirement in satisfying stringent health and safety criteria imposed by regulatory agencies, *e.g.*, in long-term nuclear waste storage applications. 2) Conventional deterministic calculations can lead to noticeable systematic biases under extreme conditions such as those found in this exercise. It is evident from Table 1 that the biases in the present example are fairly modest in comparison to the corresponding derived standard deviations. As mentioned earlier, these standard deviations account for random error in the determination of residual radioactivity. Nevertheless, it seems worthwhile under extreme conditions to avoid systematic bias effects in the derived radioactivity values by employing the suggested Monte Carlo approach rather than resorting to erroneous deterministic analysis.

10. Application to Radiation Shielding

The provision of adequate shielding is necessary to assure the safe handling and storage of radioactive nuclear materials. The assumption that attenuation of penetrating radiation in shielding materials obeys a strict exponential law represents a considerable oversimplification of the physical problem, in many instances. It fails to be exact because it ignores variations in radiation intensity and energy spectrum distortion effects due to scattering and other physical phenomena (see below). Nevertheless, the exponential assumption is sometimes invoked for the purpose of providing qualitative estimates of material requirements for shielding against penetrating neutral (uncharged) radiation such as photons and neutrons. In the present example, it is assumed that the attenuation in lead of 662-keV gamma rays emitted by the decay of ^{137}Cs is governed approximately by the formula

$$I \approx I_0 \exp(-n \sigma_T x), \quad (36)$$

where I_0 is the unshielded source strength, I is the effective exterior source strength with shielding material included (lead in this example), n is the atomic density (atoms/cm³) of lead, σ_T is the total cross section for 662-keV photons in lead, and x is the thickness of lead shielding. The structure of Eq. (36) clearly resembles that of Eq. (33). The photon cross section $\sigma_T = 38.59$ barn/atom is extracted from tables in Storm and Israel [12]. The atom density $n = 3.299 \times 10^{22}$ atoms/cm³ is deduced from the mass of the lead atom given by Tuli [10] and the mass density of lead tabulated in *CRC Handbook of Physics and Chemistry, 67th Edition* [13]. The parameter $\Sigma_T = n \sigma_T = 1.273$ cm⁻¹ is often referred to as the macroscopic total cross section. It is assumed for present purposes to have an error of 5%; no error is assigned to I_0 . The error amplification factor described in Section 3 can be derived from the equation

$$s_I / I \approx n \sigma x (s_\sigma / \sigma) = \Sigma x (s_\Sigma / \Sigma). \quad (37)$$

in the present shielding application. For convenience σ_T has been replaced by σ and Σ_T by Σ in Eq. (37). Thus, in this instance the error amplification factor is either $n \sigma x$ or Σx , depending on whether one chooses to attribute error to the microscopic cross section σ or the macroscopic cross section Σ . The latter approach combines the uncertainty in density and microscopic cross section and is probably is a more reasonable approach.

Let us suppose that the ^{137}Cs source in question is confined to a small sealed capsule (nearly a point source) and that it has an unshielded strength $I_0 = 100$ Ci. Furthermore, we stipulate that this capsule be stored in a lead container (lead pig) such that the active material is completely surrounded by 10 inches ($x = 25.4$ cm) of lead. What will be the effective source strength for emission of un-scattered gamma rays from this container? First, we note from an application of Eq. (37) – using the parameters given above – that the error amplification factor is ≈ 32 . This suggests that an error of 5% in the cross section could be amplified to $\approx 160\%$! To obtain more definitive results, we derived the effective shielded source strength I by both a deterministic calculation – as

described in Section 4 – and by Monte Carlo simulation – as discussed in Section 5. The Monte Carlo simulation was carried out using Eqs. (9) and (10), as described in Section 9. The deterministic approach yielded a transmitted radiation intensity comparable to that from an equivalent 0.9089 pCi (162%) source while the Monte Carlo simulation produced a mean value comparable source strength of 3.358 pCi (127%). The respective standard deviations (in percent) are shown in parentheses. The effective source strengths determined by these two methods differ by a factor of 3.695 for the severe conditions posed in this example. The Monte Carlo simulation also generated a discrete empirical probability distribution for $\ln I$, as described in Section 9. We tested the assumption that the natural logarithm of I is normally distributed by comparing the discrete probability distribution for $\ln I$ with an analytical normal probability density function (PDF). The results are shown in Figure 7. Although these shapes are observed to agree reasonably well over two decades of the probability function, there are some noticeable differences for smaller probability values. The overall agreement here is not as good as was encountered in the example given in Section 9. However, this is not surprising since the present example involves considerably larger errors and very severe conditions. Still – for most practical purposes – it appears to be acceptable in this specific case to assume that the probability density function that describes the transmitted radiation intensity can be approximated adequately by a lognormal function.

Unlike the case of radioactive decay that is discussed in Section 9, there is good reason, in shielding, to question the fundamental validity of the pure exponential attenuation model represented by Eq. (36). In the transport of penetrating, uncharged radiation (*e.g.*, photons and neutrons) through matter, the exponential model overestimates the attenuation (underestimates the transmission) by amounts that become increasingly important as the thickness of absorbing material increases. There are also significant spectral alterations that occur due to scattering and other physical phenomena. This is a situation where the principle culprit that leads us to calculate the wrong answer is not related to non-linearity or probability effects but rather to fundamental inappropriateness of the physical model. It is well known that there is a radiation “build up” effect that leads to an enhancement of penetrating radiation transmission relative to predictions from the exponential model [14,15]. For example, it has been shown that for copper and steel one can anticipate buildup factors approaching 3 for 6-MeV gamma rays and material thickness around 20 cm [15,16]. Various analytical formulas have been suggested for addressing this problem, and these have been included in a variety of radiation transport computer codes. Today, it is generally accepted that the best approach for dealing with radiation transport problems is Monte Carlo simulation. Only in this way is it possible to take into consideration detailed changes in the spectral characteristics of transmitted radiation that have a profound effect on calculations of physical quantities that really matter, such as energy deposition and biological dose. It should be noted that the Monte Carlo technique is potentially fully compatible with the probabilistic approach to uncertainty that is being considered in this report.

In the present study we chose not to investigate models of radiation transport more realistic than exponential attenuation. One reason for this is that the general approach would be the same; the mathematics would simply be more complicated.

Perhaps a more important reason is our belief that reliable determinations of radiation transport through materials require use of either sophisticated deterministic, multi-group transport codes or Monte Carlo simulation. If deterministic codes are used, one needs to be aware of the potential for systematic error that may result from those effects discussed in this report, if the data uncertainties are large. With Monte Carlo simulation it is possible, in principle, to avoid this problem. However, existing Monte Carlo codes tend not to include a capability for dealing with error information and, thus, would likely be equally susceptible to the problem.

(Blank Page)

11. Application to Astrophysical Nuclear Reaction Rates

A very interesting and challenging example of dealing with large errors and severe conditions involves the determination of nuclear reaction rates that are employed for astrophysical network calculations of stellar nucleosynthesis [7,17–21]. In fact, our interest in this application was the principal motivating factor that led to undertaking the present investigation.

A stellar nuclear reaction rate R is defined as the energy integral of the product of a normalized Maxwellian-Boltzmann spectrum of interaction energies, ϕ , and the reaction cross section, σ , *i.e.*,

$$R = R(T) = \int \sigma(E)\phi(E,T) dE , \quad (38)$$

where T is the stellar temperature that defines the spectrum ϕ . Since the reaction cross section can be comprised of several components, so can the reaction rate. For present purposes we will consider reactions initiated by charged particles such as protons or alpha particles. These processes tend to have very small cross sections at the relatively low particle energies (on the nuclear scale) typically encountered in stellar environments. Furthermore, the cross-section errors tend to be quite large because these cross sections are difficult – perhaps in many cases impossible – to measure directly at low energies. Although these reaction rates may be very weak, their influence on stellar evolution can be profound owing to the enormous masses of stars. Generally, the cross sections need to be estimated from nuclear model calculations or deduced indirectly from auxiliary information about nuclear structure or the properties of resonance interactions. Typically, we can express the total reaction rate reasonably well as a sum of terms, each corresponding to a conceptually distinct physical process:

$$R \approx R_{\text{sub}} + R_{\text{res}} + R_{\text{comp}} + R_{\text{dir}} . \quad (39)$$

R_{sub} identifies a contribution from bound states in the compound-nuclear system of interacting particles at excitation energies near the incident-particle separation energy. R_{res} is the contribution from discrete low-lying unbound resonances of the compound-nuclear system. It is often the dominant term of Eq. (39), especially for moderate values of stellar temperature. R_{comp} is the compound-nucleus component corresponding to higher-excitation, unresolved resonances. It is usually estimated from Hauser-Feshbach calculations, and it can become the dominant term for very high stellar temperatures. Finally, R_{dir} is the component due to direct reactions in which the colliding particles do not first form a compound nucleus. This contribution is generally relatively small and it tends to be smooth as a function of energy. The formula given in Eq. (39) is approximate in the sense that it is not possible to isolate the various labeled components completely from each other due to interference effects. Still, Eq. (39) provides a reasonably good model for handling most stellar applications. In the present example, we will assume that the reaction rate is dominated by the component due to discrete, unbound resonances, *i.e.*, that $R \approx R_{\text{res}}$. Furthermore, it is assumed that the spacing between these resonances

is considerably larger than the widths of the individual resonances, *i.e.*, $D/\Gamma \gg 1$ [17]. Under these conditions we obtain the expression

$$R \approx (1.54 \times 10^5) (\mu T_9)^{-3/2} f \sum_i S_i \exp(-11.605 E_i / T_9), \quad (40)$$

where R is the reaction rate in units of $\text{cm}^3/\text{second}/\text{mol}$, T_9 is the stellar temperature expressed in units of GK (1 GK = 10^9 Kelvin), μ is the reduced mass of the interacting particles in amu, E_i is particle interaction energy corresponding to the i^{th} resonance in MeV, and S_i is the corresponding resonance strength factor in eV [17,18,21]. The indicated sum extends over all the considered resonances. The factor “ f ” is called the electron-screening factor. It takes into account modification of the effective potential for interaction of two charged nuclear particles due to the presence of an electron cloud around the nucleus. For present purposes we assume $f = 1$ for convenience, with no relevant loss of generality.

Until recently, information on stellar nuclear reaction rates was generally employed only in deterministic calculations of stellar evolution and the synthesis of elements. Lately, a group at Oak Ridge National Laboratory has been exploring the use of Monte Carlo simulation as a tool in performing these calculations [7]. These workers incorporated existing reaction-rate information that was obtained mainly from Hauser-Feshbach calculations, *e.g.*, from Rauscher *et al.* [22] – and assumed errors of 50% – in their investigation. These values served as parameters for lognormal probability distributions that they utilized in Monte Carlo analyses. They found out that the elemental abundances derived from such calculations tend to have probability distributions that also can be represented reasonably well by lognormal functions. This, of course, is consistent with findings that have emerged from the present investigation, as indicated in earlier sections of the present paper.

In this section, we employ both hypothetical and realistic nuclear reaction data to investigate the degree to which lognormal functions can be used to describe reaction-rate probability distributions that have been derived numerically from more fundamental information – in this case from lognormally distributed resonance parameters – according to Eq (40).

First, we address the error amplification issue – as described in Section 3 – applied to astrophysical resonance reaction rates. The formula that is comparable to Eq. (12) in the present situation – as long as the errors in the resonance parameters are assumed to be uncorrelated – is

$$(s_R / R)^2 \approx \sum_i [A_{E_i}^2 (s_{E_i} / E_i)^2 + A_{S_i}^2 (s_{S_i} / S_i)^2]. \quad (41)$$

It relates the fractional error in R to the fractional errors in the resonance energies and strengths through conventional error propagation using Eq. (40). Eq. (41) differs from Eq. (12) in that it indicates the total error in R should be computed by combining all partial errors in quadrature [1]. In this formula, A_{E_i} and A_{S_i} are the partial-error amplification factors associated with each indicated variable and “ s ” denotes standard deviation.

To demonstrate the severity of the error amplification effect under certain circumstances, we examined a simple, hypothetical example that involves just two resonances. The chosen resonance parameters are: $E_1 = 0.194$ MeV and $s_{E1} = 0.003$ MeV (1.5% error); $S_1 = 4.8 \times 10^{-7}$ eV and $s_{S1} = 1.6 \times 10^{-7}$ eV (33.3% error); $E_2 = 0.305$ MeV and $s_{E2} = 0.004$ MeV (1.3% error); $S_2 = 3.7 \times 10^{-5}$ eV and $s_{S2} = 1.85 \times 10^{-5}$ eV (50% error). Specific values of A_{Ei} and A_{Si} ($i = 1, 2$) for selected stellar temperatures T_9 are given in Table 2. A great deal about the nature of this hypothetical physical problem can be learned from an examination of Table 2. Since the reaction rate is a linear function of the resonance strengths, it should be anticipated – from the discussion in Section 3 – that the corresponding amplification factors will be less than unity, *i.e.*, $A_{Si} \leq 1$. This point is clearly evident from an inspection of Table 2. The actual magnitude of A_{Si} depends on the weight given to the individual resonance by the Maxwell-Boltzmann distribution function of interacting-particle energies. Clearly, this weighting depends on stellar temperature. As we might have suspected, the only error amplification factors greater than unity correspond to the resonance energies, *i.e.*, to A_{Ei} . Again, the effect is strongly dependent on stellar temperature. When the resonances are widely spaced compared to their individual widths, only the lowest-energy resonances are capable of introducing large error amplification. From this result we can conclude that it is very important to determine the energies of the lowest unbound resonances as accurately as possible in order to be able to obtain reliable estimates for the reaction rates at low stellar temperatures.

Next, we examine a realistic problem in nuclear astrophysics in some detail. Consider the charged-particle reaction $^{31}\text{P}(p,\gamma)^{32}\text{S}$. This reaction is known to play an important role in nuclear hydrogen burning via the *rp*-process that occurs during a nova outburst or the cataclysmic death of a large star by a supernova explosion [19]. Table 3 lists the parameters for 46 known unbound resonances of this reaction with measured or estimated strengths up to proton energy $E_p \approx 2$ MeV. These data were collected from a 1990 evaluation by Endt [23], from 1993 experimental results at low energy by Iliadis *et al.* [24], and from the data compilation for this reaction by Smith and Daly [25]. The absolute resonance-energy errors were assumed to be 0.002 MeV in those cases where they are not given in the original published sources. The resonance strength errors, when not given explicitly, were assumed to be 30% except in those instances where the resonance strength was indicated to be an upper bound. Then, a 50% error was assumed.

It is instructive to examine the effects of varying stellar temperature by performing deterministic calculations for this reaction using only the five lowest-lying resonances listed in Table 3. Individual contributions from each of the first five terms in Eq. (40) are plotted in Figure 8 in bar-graph form. Separate plots are provided for nine selected values of stellar temperature. Only the first resonance contributes significantly to the reaction rate at $T_9 = 0.02$ GK, and hence at lower temperatures as well. Since Eq. (40) is dominated by a single exponential term under these conditions, we can anticipate that the present example will exhibit a probabilistic behavior similar to that described in Sections 9 and 10. At $T_9 = 0.04$ GK, the second resonance begins to have some influence. By $T_9 = 0.1$ GK, the second resonance is by far the dominant contributor to the overall

reaction rate. Since it is a relatively strong resonance, its influence continues to be felt up to $T_9 = 0.5$ GK. The third resonance is very weak and appears so close in energy to the second resonance that it has hardly any influence at the considered temperatures. For $T_9 > 0.5$ GK, the fourth and fifth resonances have the predominant influence on the reaction rate. In the broad temperature range between 1 and 10 GK there is only a modest variation in the relative contributions from the fourth and fifth resonances. The effect described here is sometimes referred to as the Gamow-Peak effect [17,18]. It comes about because of the dramatic variation in the shape of the Maxwell-Boltzmann energy distribution function with stellar temperature, particularly for lower temperatures. This analysis illustrates an important consideration for astrophysics, namely, that the impact of a particular charged-particle nuclear reaction in a stellar environment can depend very strongly on the properties of just a few of its strongest and/or lowest-lying unbound resonances.

Suppose that the reaction rate R is dominated by just a single resonance. Furthermore, let us consider $\ln R$ rather than R itself. Then, from Eq. (40) we can deduce the expression

$$\ln R \approx C(T_9) + \ln S - 11.605 E / T_9, \quad (42)$$

where $C(T_9)$ is a function of stellar temperature. However, C is not a random variable so it contributes no error to $\ln R$. In Eq. (42), only S and E are random variables with potential for error. If we assume that the resonance strength, S , is governed by a lognormal distribution, then $\ln S$ should be normally distributed. The resonance energy E is also governed by a lognormal distribution. Let us consider two extreme cases as defined by the stellar temperature. If T_9 is relatively large, then the error in $\ln R$ will be dominated by the error in $\ln S$. Hence, its probability distribution can be approximated by a normal (Gaussian) function. However, if T_9 is very small, $\ln R$ will be dominated by the term involving resonance energy, E . Then, its probability distribution can be approximated by a lognormal function. Since the error in E is generally quite small (a few percent at most), this lognormal distribution will be very close – if not exactly equal to – a normal distribution (Section 7). So, for all practical purposes we can treat this distribution as normal. This line of reasoning leads us to the conclusion that $\ln R$ should be approximated quite well by a normal distribution in most circumstances. We shall demonstrate that this is indeed the case later in this section by means of detailed Monte Carlo simulations.

Several computer codes were developed specifically for this project in order to be able to carry out both deterministic calculations (Section 4) and Monte Carlo simulations (Section 5) of $^{31}\text{P}(p,\gamma)^{32}\text{S}$ reaction rates at 29 selected stellar temperatures that span a range of nearly three decades ($T_9 = 0.011 - 9.00$ GK). The Monte Carlo analyses were performed mainly using natural logarithms of reaction rates for the reason mentioned in Section 8. Conversion to actual reaction-rate information was accomplished using Eqs. (28) and (29), in the manner described in Sections 8 – 10.

Table 4 presents the results obtained from both deterministic calculations and Monte Carlo simulations for a limited collection of stellar temperatures in order that the nature of the error correlation patterns can be exhibited more conveniently. Complete sets of the 29 reaction-rate results calculated by both methods are presented in Table 5. Plots of ratios of these results are shown in Fig. 9. There are several points to be made concerning the results presented in these two tables and the figure. It is evident that the fractional errors grow progressively larger as T_9 becomes smaller. This reflects the error amplification phenomenon discussed in Section 3. Similarly, the deviations between results generated by deterministic calculations and corresponding ones that were deduced from Monte Carlo simulation become steadily more pronounced as the stellar temperature drops. It is interesting to observe, however, that the correlation matrices obtained by these two distinct methods – while differing in fine detail – are qualitatively similar. These correlations are governed by the structure of Eq. (40). Although the Monte Carlo simulation exercises focused mainly on natural logarithms of reaction rates, it is easy to demonstrate that the correlation pattern generated for a set of values and their corresponding set of natural logarithms are the same.

Detailed probability distributions for the natural logarithm of reaction rate were also generated by the Monte Carlo method for several stellar temperatures in the range $T_9 = 0.011 - 9$ GK using the methods discussed in Sections 8 – 10. The results for $T_9 = 0.011$ and 0.1 GK are shown in Fig. 10. It is evident from Fig. 9 that the region of stellar temperature $T_9 \leq 0.1$ involves severe conditions, as defined in the present context. The linear and semi-logarithmic plots shown in Fig. 10 demonstrate that the empirical probability distributions generated by Monte Carlo simulation for the natural logarithms of resonance reaction rates can be represented very well by normal probability functions with mean values and standard deviations derived by Monte Carlo simulation (Section 5). Good agreement is apparent over three to four decades in the value of probability density. Similar good agreement was observed between empirically derived probability distributions for natural logarithms of reaction rates and equivalent normal probability functions at the other temperatures we investigated. This outcome supports the idea that the probability distributions for the reaction rates themselves should be described well by lognormal functions. It is also consistent with the observations made by Hix *et al.* in a report on their earlier work at Oak Ridge National Laboratory [7].

Since the agreement between the results obtained deterministically and by Monte Carlo simulation is generally quite good, except possibly at the lowest stellar temperatures, one might question whether these differences in reaction-rate values are really that significant. In response to this objection, we point out that a thorough understanding of these low-temperature environments is very important for the accurate analysis of many important stellar processes, including nova outbursts. Consequently, the reaction rates applicable to this temperature regime need to be determined accurately and represented properly. One of the great challenges of nuclear astrophysics is that of acquiring reaction-rate data of sufficient quality to enable relatively low-temperature stellar conditions to be modeled reliably.

Theoretical nuclear astrophysicists must deal with a large number of stellar reaction rates spanning wide ranges of stellar temperatures when they perform stellar evolution network calculations. Consequently, there is a strong motivation to represent this reaction-rate information in the form of parameterized functions of stellar temperature in order to reduce the size of input data files used by the stellar modeling codes and to enhance flexibility. One popular scheme for condensing reaction-rate information has been developed by Thielemann and his collaborators [26]. Their approach is to represent the nuclear reaction rate R versus stellar temperature T_9 by the empirical seven-parameter function

$$R \approx \exp [a_1 + a_2 T_9^{-1} + a_3 T_9^{-1/3} + a_4 T_9^{1/3} + a_5 T_9 + a_6 T_9^{5/3} + a_7 \ln(T_9)], \quad (43)$$

or, equivalently,

$$\ln R \approx a_1 + a_2 T_9^{-1} + a_3 T_9^{-1/3} + a_4 T_9^{1/3} + a_5 T_9 + a_6 T_9^{5/3} + a_7 \ln(T_9), \quad (44)$$

where the parameters a_i are selected so that this formula will yield good agreement to reaction-rate values derived by various methods, including those discussed in this report. Tables of parameters a_i have been produced by other workers using this scheme and they are available from the literature [26,27]. This concept is appealing because it offers the possibility of calculating a particular reaction rate for any desired stellar temperature within the validated fitting range by using a simple analytic function that involves just a few parameters. Such determinations can be made quickly “on the fly” during stellar evolution modeling calculations. There are two problems associated with the conventional application of this technique, based on findings from the present investigation: First, reaction-rate uncertainties are generally not considered. Second, we have demonstrated in this work that it is misleading to refer to a “unique” reaction rate for a specific stellar temperature, T_9 , at the low stellar temperatures where nuclear data uncertainties tend to be large. Instead, there is a necessity to resort to Monte Carlo simulation and the use of probability distributions to represent various reaction rates.

It is obvious from an inspection of Eq. (44) that $\ln R$ is a linear function of the parameters a_i . We suggest that the method developed by Thielemann *et al.* [26] can also be applied successfully in dealing with circumstances involving large errors and severe conditions provided that we include the errors and that the fitted quantities are interpreted as parameters of probability distributions rather than as deterministic values. The procedure is as follows: A collection of mean values and standard deviations (which we shall refer to below as “errors”) is generated by Monte Carlo simulation for the distributions of $\ln R$ using Eq. (40). These values correspond to various selected stellar temperatures that span the range of interest. For convenience, we denote the mean values to be fitted by $\langle \ln R \rangle_{\text{data}}$ and the corresponding errors by $(\text{Error } \ln R)_{\text{data}}$. Eq. (44) is fitted rigorously to the $\langle \ln R \rangle_{\text{data}}$ values by applying the linear least-square method with data-point weighting included [1,6]. We assume here, for simplicity, that these errors are not correlated. Then, individual points to be fitted are weighted by the inverse squares of their errors. Of course, the least-squares methodology allows for the error correlations that are provided automatically by Monte Carlo simulation to be included if that should

be desired. The error values resulting from Monte Carlo simulation must also be fitted. Lacking an obvious alternative fitting function, we have assumed that Eq. (44) can also be used for this purpose. However, in this instance it is not possible to weight the error values in an objective manner for the fitting procedure since the notion of an “error in the value of an error” is meaningless. To circumvent this problem, we assume arbitrarily that the errors to be fitted can be weighted equally on a percentage basis for the least-squares fitting exercise. From the fitted curves for $\langle \ln R \rangle$ and its error, values for the parameters describing the lognormal probability distributions for reaction rate R can be calculated for any value of T_9 within the validated fitting range by applying Eqs. (28) and (29) – provided that it is assumed that $\ln R$ is normally distributed.

To test this approach, we used Eq. (44) to fit mean values and errors corresponding to the distributions of $\ln R$ for the $^{31}\text{P}(p,\gamma)^{32}\text{S}$ reaction at 29 stellar temperatures, as described earlier in this section. The best-fit solution parameters, a_i , obtained from the mean-value fitting exercise are given in Table 6 along with the parameter errors and error correlations. A reasonably good fit to these data was obtained, as is demonstrated by a least-squares fit solution with chi-square per degree of freedom equal to 1.827 [1,6]. Of course, it was anticipated that a decent fit could be achieved since the functional form of Eq. (44) was developed by Thielemann *et al.* [26] explicitly for the purpose of fitting reaction-rate data of this nature. A detailed comparison of the mean-value data points, $\langle \ln R \rangle_{\text{data}}$, and corresponding values, $\langle \ln R \rangle_{\text{fit}}$, derived from the fitted curve is provided in Table 7, and a corresponding quality-of-fit indicator is plotted in Fig. 11. This indicator is obtained by dividing the difference between the data point and its corresponding value from the fitted curve by the error in the fitted data point; it can be either positive or negative (if not zero). An indicator value of unity implies that a data point and corresponding value from the curve differ by an amount exactly equal to the data point error. It is evident that there is a systematic trend to the deviations; this is not surprising given that Eq. (44) is an empirical formula. Nevertheless, it is seen that only 11 of the 29 fitted data points deviate from the curve by more than their error (one standard deviation). This is reasonably consistent with the fact that $\approx 32\%$ of these data points should be expected to differ by more than one standard deviation from the curve if their scatter were governed by purely random statistical effects (see Table 7.1 of Ref. [1]). We also generated a least-squares fit of Eq. (44) to the error information, $(\text{Error } \ln R)_{\text{data}}$, given in Table 7, although there was no *a priori* reason to expect that this formula would be applicable to a fitting exercise for which it was not designed. To satisfy data input requirements for the least-squares procedure that was used, dummy “errors” of 10% were assigned to each of the error values to be fitted. This 10% error figure was selected after some trial and error. This led to a least-squares fit solution with chi-square per degree of freedom parameter equal to 1.403. This is a very respectable outcome. A detailed comparison of the error data points, $(\text{Error } \ln R)_{\text{data}}$, and values from the fitted curve, $(\text{Error } \ln R)_{\text{fit}}$, is provided in Table 7 and a corresponding quality-of-fit indicator is plotted in Fig. 11. This indicator is defined in the manner described above. Again, some systematic effects are observed for the deviations. However, only 5 of the fitted data points deviate from the curve by more than 10%. These two fitting exercises demonstrate that it is possible to represent detailed information about reaction-rate probability distributions quite adequately – over a range of stellar temperatures that spans

nearly three decades ($T_9 = 0.011 - 9$ GK) – by using the formalism of Thielemann *et al.* and only 14 parameters (seven for the mean values and seven for the errors).

Astrophysicists are interested in information on reaction rates, R , for their stellar evolution calculations. Results for $\ln R$ are not directly useful. Of course, it would be perfectly reasonable to provide information only for $\ln R$ and then convert this to information for the equivalent R during the stellar evolution calculations, “on the fly”, utilizing Eqs. (28) and (29). We have explored this issue in the context of the present example that deals with $^{31}\text{P}(p,\gamma)^{32}\text{S}$ reaction rates. Values of $\langle \ln R \rangle_{\text{data}}$ and $(\text{Error } \ln R)_{\text{data}}$ were converted to equivalent $\langle R \rangle_{\text{data}}$ and $(\text{Error } R)_{\text{data}}$ using Eqs. (28) and (29). The same procedure was used to convert corresponding values of $\langle \ln R \rangle_{\text{fit}}$ and $(\text{Error } \ln R)_{\text{fit}}$ to equivalent $\langle R \rangle_{\text{fit}}$ and $(\text{Error } R)_{\text{fit}}$. The results from this analysis appear in Table 8. Quality-of-agreement indicators that quantify these differences are plotted in Fig. 11. Although there are again some systematic effects evident in this comparison, the overall agreement is quite good. It is seen that the differences between values derived from Monte Carlo simulations and those obtained from the fitting exercises exceed their errors for only 10 of the 29 plotted data points.

12. A Final Look at Errors and the Effects of Non-linearity

There is a common characteristic to the results obtained from analyses of the examples given in Sections 9 – 11. The mean values of the derived quantities obtained by Monte Carlo simulation using lognormal distributions for the primary random variables tend to be larger than the corresponding values obtained by deterministic substitution. The larger the error – or the more extreme the conditions encountered – the larger the observed biases. This raises a question as to whether this is a universal effect or whether it depends in a specific way on the nature of the probability distribution and/or non-linear function under consideration.

Upon closer examination of each of the examples considered in Sections 9 – 11, particularly in the extreme limits, we see that basically we are dealing with functions of the form

$$y = f(x) = \exp(- a x) \quad (x > 0; a > 0). \quad (45)$$

In this case,

$$\langle y \rangle = \int f(x) p(x) dx. \quad (46)$$

There is no particular need to generate an explicit probability distribution for y [1]. Following the discussion in Section 3, it is evident that the error amplification factor is “ ax ” for this function.

It is possible to compare values of $\langle y \rangle$ and $y = f(m_x)$ – where $m_x = 6$ is the mean value of the lognormal probability distribution $p(x)$ that applies to the primary random variable x – by using a spreadsheet program for the analysis. There is no need in this instance to resort to Monte Carlo simulation to evaluate Eq. (46), although this approach could, of course, be applied and it would lead to the same result. In the upper half of Table 9, values for the ratio of $\langle y \rangle$ to $f(m_x)$ are given for $a = 1$ and various values of the standard deviation s_x in x equivalent to 1, 2, 5, 10, 20, 50, and 100% error. The value $a = 1$ does not constitute an extreme condition, so this exercise tests the effects of error size on the results. However, it should be noted that the error amplification factor is 6 for this part of the table. The lower half of Table 9 gives similar results for the case where s_x corresponds to 5% (a very modest error) but $a = 0.1, 0.2, 0.5, 1, 2, 5,$ and 10 . The larger values of “ a ” correspond to extreme conditions. In this part of the table, the error amplification factor ranges from 0.6 to 60. It is clear from the results given in this table that there is a bias toward $\langle y \rangle$ being larger than $f(m_x)$. This bias becomes insignificant when the error is small and the conditions are not extreme. Would the effect be the same if a Gaussian probability distribution were used rather than the lognormal distribution? Due to the fact that there is a significant probability of encountering negative (non-physical) values of x for Gaussian distributions with large errors, it is really not meaningful to explore this possibility any further.

Instead, we examine what happens if a different non-linear function is involved. For this purpose, we consider the function

$$y = f(x) = \exp(-a / x) \quad (x > 0; a > 0). \quad (47)$$

The function indicated in Eq. (47) behaves quite differently from the function defined by Eq. (45). Following the discussion in Section 3, it is evident that the error amplification factor is “ a/x ” for this function. For small x the values of y become small while for large x the value of y approaches unity. This is just the opposite behavior of Eq. (45). Table 10 gives results of a numerical exercise similar to the one that generated Table 9. The observed biases are quite different in this case. Considering the upper half of Table 10, the bias due to increasing error size, with fixed $a = 1$, is in the opposite direction from that seen in Table 9. Furthermore, these biases are relatively modest. For this part of the table, the error amplification factor is approximately 0.167. Considering the lower half of Table 10, the bias generated by fixing the error at 5% but increasing “ a ”, and thus the extreme nature of the problem, the biases are in the same direction as observed for the corresponding exercise documented in Table 9. However, once again these biases are relatively modest. The error amplification factor ranges from approximately 0.0167 to 16.7.

So, it is clear that the nature of the non-linear function under consideration has a profound impact on both the magnitude and direction of the biases generated when the errors become large or the conditions extreme. Therefore, it would seem to be impossible to generalize about the outcome for other non-linear functions. Each individual situation has to be examined independently to reveal the basic characteristics inherent to the particular non-linearity in question. In passing, it should be noted that the behavior of the error amplification factor gives us a strong indication as to the influence that non-linearity of a particular function will have on producing biases when the errors are large or the conditions are extreme (or both).

13. Concluding Remarks

The following observations concerning the present investigation can be offered as conclusions:

- 1) In physical situations involving large errors and/or extreme conditions the use of deterministic calculations to relate derived information to more fundamental data can lead to biased results. Instead, a probabilistic approach should be applied in which both the basic parameters and the derived results are represented by probability distribution functions.
- 2) Knowledge about the fundamental nature of a particular random variable plus some specific numerical information about that variable, including estimates of the mean value and standard deviation, can guide the selection of an appropriate probability distribution to represent it in ensuing analysis that involves that variable. For example, when a physical quantity can be represented by a random variable that is allowed to assume any value between $-\infty$ and $+\infty$ – and the only information available is an estimate of the mean value and standard deviation (error) – then a normal (Gaussian) probability distribution is the optimal choice to represent that variable. However, if the physical quantity is inherently positive – and the only information available is an estimate of the mean value and standard deviation – then a lognormal distribution is the optimal choice to represent the associated random variable.
- 3) Extreme conditions can lead to error amplification if the functional relationship between the primary quantity and the derived one is non-linear.
- 4) If the functional relationship between primary and derived variables is well known – and the probability distribution for the primary variable is specified – then an estimate of the “true” probability distribution for the derived variable can be generated empirically by Monte Carlo simulation to a degree of precision limited only by statistical considerations. Various low-order moments of this distribution can also be estimated by this method. If the family of probability functions to which this distribution belongs can be established from fundamental considerations, then these moments can be used to uniquely characterize the probability function.
- 5) Three important physical problems – radioactive decay, radiation shielding, and stellar reaction rates dominated by resonance phenomena – were examined in the present work. The outcome from this investigation has led us to conclude that lognormal probability functions can be employed with confidence to provide acceptable approximations to the empirical probability distributions generated by Monte Carlo for those derived parameters that are known *a priori* to be inherently positive in nature.

- 6) In those cases where there are large errors involved and, consequently, the lognormal distributions are severely asymmetric, we have demonstrated that the analysis required to estimate the parameters of these distributions can be carried out best using natural logarithms of the random variables. This will lead to normal distributions whose parameters can be estimated with good precision by Monte Carlo simulation and then used subsequently to calculate parameters for the equivalent lognormal distributions that describe the actual random variables themselves.
- 7) The lognormal distribution appears to provide quite a good approximation – in situations involving large errors and extreme conditions – to those distributions obtained empirically from Monte Carlo simulation for the inherently positive derived quantities considered in this investigation. However, there is evidence (see Figs. 6, 7, and 10) that the agreement is not perfect – especially in the wings of these distributions far from the mean-value position. Therefore, it cannot be ruled out in certain instances that unacceptable biases would develop when the lognormal distribution is substituted for the true distribution. Approximation of the true distribution – in numerical form – by an analytical function is an expedient approach that can be very convenient. However, it should be implemented only in those situations where the impact of this approximation is minimal.
- 8) The effects of the interplay of non-linearity and larger errors cannot be generalized. The size and even direction of differences between mean values and errors deduced by deterministic calculations and those obtain by Monte Carlo simulation is found to depend profoundly on the nature of the non-linear function involve in the analysis.

Acknowledgements

The authors are indebted to Dr. William Raphael Hix and Dr. Michael S. Smith, Oak Ridge National Laboratory, U.S.A., and to Dr. Friedrich H. Froehner, Forschungszentrum Karlsruhe, Germany, for their valuable comments pertaining to this work. The U.S. Department of Energy, Science Programs, supported this investigation under Contract W-31-109-Eng-38. One of the authors (LVW) also acknowledges support from the U.S. Department of Energy, Science Programs, under Grant DE-FG02-99ER41116.

(Blank Page)

References

- [1] D.L. Smith, *Probability, Statistics, and Data Uncertainties in Nuclear Science and Technology*, OECD Nuclear Energy Agency Nuclear Data Committee Series “Neutron Physics and Nuclear Data in Science and Technology”: Volume 4, American Nuclear Society, LaGrange Park, Illinois, U.S.A. (1991).
- [2] E.T. Jaynes, *Papers on Probability, Statistics, and Statistical Physics*, R.D. Rosencrantz, Ed., Reidel Publishing Company, Dordrecht, Netherlands (1983).
- [3] F.H. Froehner, *Nuclear Science and Engineering* **126**, 1 (1997).
- [4] C.E. Shannon, *Bell Systems Technology Journal* **27**, 379 (1948).
- [5] H. Jeffreys, *Theory of Probability*, Clarendon Press, Oxford (1939).
- [6] D.L. Smith, “A Least-squares Computational ‘Tool Kit’ ”, Report ANL/NDM-128, Argonne National Laboratory, Argonne, Illinois, U.S.A. (1993). This report is available from the Internet: <http://www.td.anl.gov/reports/ANLNDMReports.html>.
- [7] W.R. Hix, M.S. Smith, A. Mezzacappa, S. Starfield, and D.L. Smith, “The Impact of Nuclear Reaction Rate Uncertainties on Evolutionary Studies of the Nova Outburst”, 10th Annual October Astrophysics Conference in Maryland: Cosmic Explosions!, College Park, Maryland, October 11-13, 1999.
- [8] W.H. Press, S.A. Teukolsky, W.T. Vetterling, and B.P. Flannery, *Numerical Recipes in FORTRAN: The Art of Scientific Computing – 2nd Edition*, Cambridge University Press, Cambridge, England (1992).
- [9] E. Browne and R.B. Firestone, *Table of Radioactive Isotopes*, John Wiley & Sons, New York (1986).
- [10] J.K. Tuli, “Nuclear Wallet Cards”, National Nuclear Data Center, Brookhaven National Laboratory, Upton, New York (2000). This material is available from the Internet: <http://www.nndc.bnl.gov/wallet/>.
- [11] D.L. Smith and A. Fessler, *Radiochimica Acta* **79**, 1 (1997).
- [12] E. Storm and H.I. Israel, *Nuclear Data Tables* **A7**, 565 (1970).
- [13] R.C. Weast, Editor, *CRC Handbook of Chemistry and Physics, 67th Edition*, CRC Press, Inc., Boca Raton, Florida (1986).
- [14] A.B. Chilton, “Broad Beam Attenuation”, *Engineering Compendium on Radiation Shielding Vol. 1: Shielding Fundamentals and Methods*, Eds. R.G. Jaeger, E.P. Blizzard,

A.B. Chilton, M. Grotenhuis, A. Holenig, Th.A. Jaeger, and H.H. Eisenlohr, Springer-Verlag, Berlin, p. 202 (1968).

[15] M.J. Berger and D.J. Rose, *Radiation Research* **12**, 20 (1960). Also see National Bureau of Standards Report 5982, 2nd Edition, National Bureau of Standards (NIST), Washington, DC (1960).

[16] Y. Ikeda, Y. Uno, F. Maekawa, D.L. Smith, I.C. Gomes, R.C. Ward, and A.F. Filatenkov, “An Investigation of the activation of Water by D-T Fusion Neutrons and Some Implications for Fusion Reactor Technology”, *Fusion Engineering and Design* **37**, 107 (1997).

[17] D. Clayton, *Principles of Stellar Evolution and Nucleosynthesis*, University of Chicago Press, Chicago (1983).

[18] C. Rolfs and W. Rodney, *Cauldrons in the Cosmos*, University of Chicago Press, Chicago (1988).

[19] A.E. Champagne and M. Wiescher, “Explosive Hydrogen Burning”, *Annual Reviews of Nuclear and Particle Science* **42**, 39 (1992).

[20] C. Angulo, M. Arnould, M. Rayet, P. Descouvemont, D. Baye, C. Leclercq-Willain, A. Coc, S. Barhoumi, P. Aguer, C. Rolfs, R. Kunz, J.W. Hammer, A. Mayer, T. Paradellis, S. Kossionides, C. Chronidou, K. Spyrou, S. Degl’Innocenti, G. Fiorentini, B. Ricci, S. Zavatarelli, C. Providencia, H. Wolters, J. Soares, C. Grama, J. Rahighi, A. Shotter, and M. Laméhi Rachti, *Nuclear Physics* **A656**, 3 (1999).

[21] D.L. Smith and L.A. Van Wormer, “Nuclear Data Evaluation for Explosive Hydrogen Burning on A = 30-50 Nuclei”, *Second Oak Ridge Symposium on Atomic and Nuclear Astrophysics*, 2-6 December 1997, Oak Ridge, Tennessee, A. Mezzacappa, Editor, Institute of Physics Publishing Company, Bristol, United Kingdom (1998).

[22] T. Rauscher, F.-K. Thielemann, and K.-L. Kratz, *Nuclear Physics* **A621**, 331 (1997).

[23] P.M. Endt, *Nuclear Physics* **A521**, 1 (1990).

[24] C. Iliadis, J. Goerres, J.G. Ross, K.W. Scheller, M. Wiescher, C. Grama, Th. Schange, H.P. Trautvetter, and H.C. Evans, *Nuclear Physics* **A559**, 83 (1993).

[25] D.L. Smith and J.T. Daly, “A Compilation of Information on the $^{31}\text{P}(p,\gamma)^{32}\text{S}$ Reaction and Properties of Excited Levels in ^{32}S ”, Report ANL/NDM-140, Argonne National Laboratory (2000). This report is available from the Internet: <http://www.td.anl.gov/reports/ANLNDMReports.html>.

[26] F.-K. Thielemann, M. Arnould, and J.W. Truran, *Advances in Nuclear Astrophysics*, Eds. E. Vangioni-Flam, J. Audouze, M. Casse, J.-P. Chieze, and J. Tran Thanh Van, Editions Frontieres, Gif-sur-Yvette, France, 525 (1987).

[27] F.-K. Thielemann, M. Wiescher, and Ch. Freiburghaus, “Tables of Nuclear Reaction Rates” (1991). Data are based on Ref. W and were updated to $Z = 46$ in 1995 by Ch. Freiburghaus. This material is available from the Internet: <http://isotopes.lbl.gov/isotopes/astro/friedel.html>.

(Blank Page)

Table 1: Results obtained from calculations of residual ^{53}V radioactivity A and its associated uncertainty following an elapsed time $t = 3600$ seconds ^a

λ (sec ⁻¹) ^b	0.007220 (2.5%)	0.007502 (1.2%)	Ratio ^c
Deterministic Calculations	5.150 (65.0%) pCi ^d	1.866 (32.1%) pCi ^d	2.760
Monte Carlo Simulation	6.361 (72.5%) pCi ^d	1.965 (33.0%) pCi ^d	3.226
Ratio ^e	1.235	1.053	---

^a Analyses were performed using both deterministic calculations (Section 4) and Monte Carlo simulation (Section 5). Details are discussed in Section 9. An initial activity $A_0 = 1$ Ci is assumed (with no error). Values obtained from the Monte Carlo simulation should be interpreted as mean values of probability distributions. The quantities that appear in parentheses correspond to standard deviations expressed in percent.

^b λ is obtained using Eq. (34) and two different values of ^{53}V half life, as indicated in Section 9. Half-life errors are included in the analyses.

^c Ratios of comparable residual activities calculated using two distinct values for the decay constant λ .

^d Source intensity A after elapsed time $t = 3600$ seconds is given in units of pico Curie (1 pCi = 10^{-12} Ci).

^e Ratio of comparable residual activities calculated by the deterministic and Monte Carlo methods.

Table 2: Error amplification factors for a two-resonance reaction rate problem ^a

T_9 (GK)	A_{E1}	A_{S1}	A_{E2}	A_{S2}
0.01	225.1	1.000	≈ 0	≈ 0
0.02	112.6	1.000	≈ 0	≈ 0
0.05	45.03	1.000	≈ 0	≈ 0
0.1	22.51	0.9998	0.0069	0.0002
0.2	10.02	0.8905	1.938	0.1095
0.5	0.6561	0.1457	6.048	0.8543
1	0.1011	0.0449	3.381	0.9551
2	0.0271	0.0241	1.727	0.9759
5	0.0074	0.0165	0.6962	0.9835

^a This problem is discussed in Section 11. Resonance parameters: $E_1 = 0.194$ MeV and $s_{E1} = 0.003$ MeV (1.5% error); $S_1 = 4.8 \times 10^{-7}$ eV and $s_{S1} = 1.6 \times 10^{-7}$ eV (33.3% error); $E_2 = 0.305$ MeV and $s_{E2} = 0.004$ MeV (1.3% error); $S_2 = 3.7 \times 10^{-5}$ eV and $s_{S2} = 1.85 \times 10^{-5}$ eV (50% error). The reaction rate R is calculated using Eq. (40)

Table 3: Resonance parameters corresponding to 46 known unbound states of ^{32}S excited by the $^{31}\text{P}(p,\gamma)^{32}\text{S}$ reaction for incident proton energies up to $E_p \approx 2$ MeV. ^a

E_p ^b	s_{Ep} ^c	S ^d	s_S ^e
0.164	0.002	1.00×10^{-10}	5.00×10^{-11}
0.200	0.002	4.80×10^{-7}	1.60×10^{-7}
0.207	0.002	3.30×10^{-9}	1.65×10^{-9}
0.315	0.002	3.70×10^{-5}	1.85×10^{-5}
0.342	0.002	6.10×10^{-5}	3.05×10^{-5}
0.355	0.002	4.20×10^{-3}	7.00×10^{-4}
0.383	0.002	6.00×10^{-5}	1.20×10^{-5}
0.403	0.002	4.50×10^{-4}	7.00×10^{-5}
0.439	0.002	0.025	0.004
0.541	0.002	0.12	0.02
0.619	0.002	1.10×10^{-3}	2.00×10^{-4}
0.6424	0.0007	0.06	0.01
0.8113	0.0005	0.25	0.0375
0.821	0.001	0.05	0.015
0.8743	0.0005	0.0325	0.00975
0.8878	0.0005	0.02	0.006
0.8945	0.0005	0.08	0.024
0.9838	0.001	0.02	0.006
1.016	0.003	0.0075	0.00225
1.0565	0.0006	0.125	0.0375
1.0896	0.0006	0.0425	0.01275
1.1207	0.0006	0.35	0.105
1.1500	0.0007	0.0275	0.0075
1.1505	0.0007	0.25	0.05
1.1551	0.0006	0.17	0.051
1.2514	0.0006	1.075	0.125
1.2799	0.0008	0.0275	0.00825
1.4001	0.0006	0.1475	0.04425
1.4029	0.0008	0.575	0.1725
1.4114	0.0006	0.2275	0.06825
1.4383	0.0007	1.25	0.375
1.4700	0.0015	0.0175	0.00525
1.4731	0.0006	0.275	0.0825
1.4753	0.0015	0.0425	0.01275
1.5566	0.0006	1.025	0.3075
1.5829	0.0006	0.90	0.27
1.6989	0.001	0.1025	0.03075
1.7642	0.001	0.1025	0.03075
1.7961	0.001	0.125	0.0375
1.8915	0.001	0.25	0.075
1.8960	0.001	0.275	0.0825
1.9540	0.001	0.80	0.24
1.9771	0.001	0.45	0.135
1.9836	0.001	0.90	0.27
1.9909	0.001	0.60	0.18
2.0266	0.001	1.70	0.51

^a Resonance-parameter data are extracted from Refs. [23,24,25].

^b Resonance proton energy (MeV).

^c Standard deviation in resonance proton energy (MeV).

^d Resonance strength (eV).

^e Standard deviation in resonance strength (eV).

Table 4: $^{31}\text{P}(p,\gamma)^{32}\text{S}$ reaction rates and error correlations for six stellar temperatures

Reaction rates:

T_9 (GK)	$R_{\text{det}}^{\text{a}}$	Error R_{det} (%) ^b	$\langle R \rangle^{\text{c}}$	Error $\langle R \rangle$ (%) ^d	Ratio ^e
0.02	2.6538×10^{-44}	126	5.2091×10^{-44}	195	1.9629
0.07	1.7856×10^{-14}	43.6	1.8850×10^{-14}	44.7	1.0557
0.25	5.1511×10^{-4}	14.6	5.1732×10^{-4}	14.6	1.0043
1	83.192	9.1	83.211	9.0	1.0002
3	2516.6	5.3	2516.6	5.3	≈ 1
9	10528	6.2	10528	6.2	≈ 1

Uncertainty correlations for the deterministic calculation of reaction rates^f:

T_9 (GK)	0.02	0.07	0.25	1	3	9
0.02	100.0					
0.07	8.7	100.0				
0.25	≈ 0	22.7	100.0			
1	≈ 0	≈ 0	27.5	100.0		
3	≈ 0	≈ 0	5.4	60.9	100.0	
9	≈ 0	≈ 0	0.6	10.1	67.0	100.0

Uncertainty correlations for the Monte Carlo calculation of reaction rates^f:

T_9 (GK)	0.02	0.07	0.25	1	3	9
0.02	100.0					
0.07	10.0	100.0				
0.25	0.1	22.5	100.0			
1	≈ 0	≈ 0	27.7	100.0		
3	0.1	0.1	5.5	60.8	100.0	
9	0.2	0.1	0.7	10.2	67.1	100.0

^a Deterministic reaction rates, R_{det} , in units of $\text{cm}^3/\text{second}/\text{mol}$ are calculated directly using Eq. (40) and the resonance parameters from Table 3 (Sections 4 and 11).

^b Errors (standard deviations) in the deterministic reaction rates, Error R_{det} , are calculated directly by matrix error propagation (Sections 4 and 11).

^c Mean values of reaction rates, $\langle R \rangle$, in units of $\text{cm}^3/\text{second}/\text{mol}$ are deduced indirectly from Monte Carlo simulation using Eq. (40) and resonance parameters from Table 3 (Sections 5 and 11). Use is made of the transformation formulas given in Eqs. (28) and (29).

^d Errors (standard deviations) in the mean values of reaction rates, Error $\langle R \rangle$, are deduced indirectly from Monte Carlo simulation at the same time that $\langle R \rangle$ is determined (Sections 5 and 11).

^e Ratios of reaction-rate values $\langle R \rangle$ divided by corresponding deterministic values R_{det} .

^f Error correlations are given in percent. These matrices are symmetric so the upper halves are not shown.

Table 5: $^{31}\text{P}(p,\gamma)^{32}\text{S}$ reaction rates for 29 selected stellar temperatures

T_9 (GK)	$R_{\text{det}}^{\text{a}}$	Error R_{det} (%) ^b	$\langle R \rangle^{\text{c}}$	Error $\langle R \rangle$ (%) ^d	Ratio ^e
0.011	9.9904×10^{-78}	217	9.2754×10^{-77}	1033	9.284
0.012	1.6021×10^{-71}	200	1.0421×10^{-70}	720	6.505
0.013	2.8249×10^{-66}	185	1.3931×10^{-65}	542	4.932
0.014	8.7954×10^{-62}	173	3.4818×10^{-61}	431	3.959
0.015	6.8439×10^{-58}	163	2.2691×10^{-57}	357	3.316
0.02	2.6538×10^{-44}	126	5.2091×10^{-44}	195	1.963
0.025	3.5010×10^{-36}	105	5.3897×10^{-36}	140	1.539
0.03	8.6607×10^{-31}	91.7	1.1662×10^{-30}	111	1.347
0.04	4.9330×10^{-24}	67.7	5.7882×10^{-24}	71.1	1.173
0.05	8.9546×10^{-20}	44.1	9.9652×10^{-20}	47.0	1.113
0.06	1.0102×10^{-16}	43.3	1.0876×10^{-16}	44.8	1.077
0.07	1.7856×10^{-14}	43.6	1.8850×10^{-14}	44.7	1.056
0.09	1.8353×10^{-11}	41.2	1.8971×10^{-11}	42.1	1.034
0.1	2.0505×10^{-10}	39.9	2.1064×10^{-10}	40.7	1.027
0.15	2.7029×10^{-7}	34.2	2.7345×10^{-7}	34.2	1.012
0.2	1.7853×10^{-5}	18.4	1.7972×10^{-5}	18.2	1.007
0.25	5.1511×10^{-4}	14.6	5.1732×10^{-4}	14.6	1.004
0.3	6.1458×10^{-3}	13.7	6.1640×10^{-3}	13.7	1.003
0.4	0.15579	11.4	0.15605	11.4	1.002
0.6	4.6840	9.4	4.6875	9.4	1.001
0.9	51.010	9.1	51.026	9.1	≈ 1
1	83.192	9.1	83.211	9.0	≈ 1
1.5	380.87	8.1	380.91	8.0	≈ 1
2	896.74	6.7	896.77	6.7	≈ 1
2.5	1621.4	5.7	1621.5	5.7	≈ 1
3	2516.6	5.3	2516.6	5.3	≈ 1
4	4542.5	5.3	4542.6	5.3	≈ 1
6	8054.0	5.8	8054.1	5.7	≈ 1
9	10528	6.2	10528	6.2	≈ 1

^a Deterministic reaction rates, R_{det} , in units of $\text{cm}^3/\text{second}/\text{mol}$ are calculated directly using Eq. (40) and the resonance parameters from Table 3 (Sections 4 and 11).

^b Errors (standard deviations) in the deterministic reaction rates, Error R_{det} , are calculated directly by matrix error propagation (Sections 4 and 11).

^c Mean values of reaction rates, $\langle R \rangle$, in units of $\text{cm}^3/\text{second}/\text{mol}$ are deduced indirectly from Monte Carlo simulation using Eq. (40) and resonance parameters from Table 3 (Sections 5 and 11). Use is made of the transformation formulas given in Eqs. (28) and (29).

^d Errors (standard deviations) in the mean values of reaction rates, Error $\langle R \rangle$, are deduced indirectly from Monte Carlo simulation at the same time that $\langle R \rangle$ is determined (Sections 5 and 11).

^e Ratios of reaction-rate values, $\langle R \rangle$, divided by corresponding deterministic values, R_{det} .

Table 6: Values of the best-fit solution parameters a_i generated by fitting Eq. (44) to natural logarithm of $^{31}\text{P}(p,\gamma)^{32}\text{S}$ reaction-rate data for 29 selected stellar temperatures ^a

Best-fit solution parameters for natural logarithm of reaction rate:

Index i	a_i	Absolute Error in a_i
1	108.511	9.80799
2	-2.33193	0.0925378
3	64.0459	8.09397
4	-177.951	18.9085
5	13.0491	1.51436
6	-0.883195	0.111885
7	71.5903	7.56445

Error correlations for best-fit solution parameters ^b:

Index i	1	2	3	4	5	6	7
1	100.0						
2	-84.6	100.0					
3	94.0	-97.2	100.0				
4	-99.0	91.2	-98.0	100.0			
5	99.6	-84.8	93.6	-98.6	100.0		
6	-98.0	79.0	-88.8	95.7	-99.1	100.0	
7	97.1	-94.4	99.4	-99.5	96.6	-92.7	100.0

^a Method is discussed in Section 11.

^b Correlations are given in percent. The matrix is symmetric so the upper half is not shown.

Table 7: Results obtained by fitting Eq. (44) to the natural logarithms of the $^{31}\text{P}(p,\gamma)^{32}\text{S}$ reaction rates and to their errors for 29 selected stellar temperatures ^a

T_9 (GK)	$\langle \ln R \rangle_{\text{data}}^{\text{b}}$	$(\text{Error } \ln R)_{\text{data}}^{\text{c}}$	$\langle \ln R \rangle_{\text{fit}}^{\text{d}}$	$(\text{Error } \ln R)_{\text{fit}}^{\text{e}}$
0.011	-177.41	2.1657	-177.80	2.1291
0.012	-163.12	1.9942	-163.29	1.9681
0.013	-151.04	1.8497	-151.06	1.8310
0.014	-140.69	1.7265	-140.62	1.7126
0.015	-131.73	1.6203	-131.61	1.6093
0.02	-100.45	1.2547	-100.24	1.2425
0.025	-81.747	1.0421	-81.529	1.0174
0.03	-69.324	0.89894	-69.041	0.86475
0.04	-53.708	0.63940	-53.296	0.67033
0.05	-43.850	0.44522	-43.656	0.55145
0.06	-36.847	0.42638	-37.061	0.47114
0.07	-31.692	0.42648	-32.212	0.41324
0.09	-24.768	0.40322	-25.458	0.33537
0.1	-22.356	0.39132	-22.980	0.30795
0.15	-15.166	0.33176	-14.942	0.22537
0.2	-10.942	0.18048	-10.368	0.18410
0.25	-7.5767	0.14533	-7.3225	0.15942
0.3	-5.0977	0.13621	-5.1129	0.14302
0.4	-1.8635	0.11354	-2.0798	0.12249
0.6	1.5410	0.093553	1.3523	0.10151
0.9	3.9287	0.090485	3.9062	0.086288
1	4.4178	0.08991	4.4403	0.082929
1.5	5.9398	0.080107	6.0680	0.071490
2	6.7970	0.066544	6.8913	0.064544
2.5	7.3899	0.057077	7.4045	0.059887
3	7.8297	0.052921	7.7772	0.056714
4	8.4203	0.052713	8.3347	0.053345
6	8.9928	0.057184	9.0798	0.053714
9	9.2599	0.061605	9.2388	0.062684

^a The method of linear least squares is employed in this analysis [1,6]. Mean values of $\ln R$ at various stellar temperatures are weighted by their standard deviations (Section 11).

^b $\langle \ln R \rangle_{\text{data}}$ represents the fitted data points.

^c $(\text{Error } \ln R)_{\text{data}}$ represents standard deviations (errors) used to weight the fitted data points.

^d $\langle \ln R \rangle_{\text{fit}}$ represents mean values calculated using Eq. (44) and parameters obtained from fitting the mean value data points.

^e $(\text{Error } \ln R)_{\text{fit}}$ represents errors calculated using Eq. (44) and parameters obtained from fitting the error data points.

Table 8: Derived values of reaction rate R from results obtained by fitting Eq. (44) to natural logarithm of $^{31}\text{P}(p,\gamma)^{32}\text{S}$ reaction-rate data for 29 selected stellar temperatures

T_9 (GK)	$\langle R \rangle_{\text{data}}^{\text{a}}$	(Error R) $_{\text{data}}$ in % ^b	$\langle R \rangle_{\text{fit}}^{\text{c}}$	(Error R) $_{\text{fit}}$ in % ^d
0.011	9.3859×10^{-77}	1039	5.8517×10^{-77}	959
0.012	1.0531×10^{-70}	724	8.4365×10^{-71}	686
0.013	1.4062×10^{-65}	544	1.3247×10^{-65}	525
0.014	3.5112×10^{-61}	433	3.6682×10^{-61}	422
0.015	2.2866×10^{-57}	358	2.5478×10^{-57}	351
0.02	5.2372×10^{-44}	196	6.3029×10^{-44}	192
0.025	5.4120×10^{-36}	140	6.5657×10^{-36}	135
0.03	1.1702×10^{-30}	112	1.5076×10^{-30}	105
0.04	5.8030×10^{-24}	71.1	8.9388×10^{-24}	75.3
0.05	9.9848×10^{-20}	46.8	1.2772×10^{-19}	59.6
0.06	1.0894×10^{-16}	44.7	8.9702×10^{-17}	49.9
0.07	1.8879×10^{-14}	44.7	1.1157×10^{-14}	43.2
0.09	1.8995×10^{-11}	42.0	9.2906×10^{-12}	34.5
0.1	2.1089×10^{-10}	40.7	1.0982×10^{-10}	31.5
0.15	2.7372×10^{-7}	34.1	3.3258×10^{-7}	22.8
0.2	1.7987×10^{-5}	18.2	3.1946×10^{-5}	18.6
0.25	5.1767×10^{-4}	14.6	6.6898×10^{-4}	16.0
0.3	6.1678×10^{-3}	13.7	6.0806×10^{-3}	14.4
0.4	0.15614	11.4	0.12589	12.3
0.6	4.6899	9.4	3.8863	10.2
0.9	51.048	9.1	49.893	8.6
1	83.247	9.0	85.089	8.3
1.5	381.07	8.0	432.93	7.2
2	897.16	6.7	985.73	6.5
2.5	1622.2	5.7	1646.3	6.0
3	2517.8	5.3	2389.3	5.7
4	4544.8	5.3	4171.9	5.3
6	8058.1	5.7	8788.4	5.4
9	10528	6.2	10309	6.3

^a $\langle R \rangle_{\text{data}}$ is calculated from $\langle \ln R \rangle_{\text{data}}$ and (Error $\ln R$) $_{\text{data}}$ using Eqs. (28) and (29).

^b (Error R) $_{\text{data}}$ is calculated from $\langle \ln R \rangle_{\text{data}}$ and (Error $\ln R$) $_{\text{data}}$ using Eqs. (28) and (29).

^c $\langle R \rangle_{\text{fit}}$ is calculated from $\langle \ln R \rangle_{\text{fit}}$ and (Error $\ln R$) $_{\text{fit}}$ using Eqs. (28) and (29).

^d (Error R) $_{\text{fit}}$ is calculated from $\langle \ln R \rangle_{\text{fit}}$ and (Error $\ln R$) $_{\text{fit}}$ using Eqs. (28) and (29).

Table 9: The effects of error and error amplification for the simple non-linear function $y = f(x) = \exp(-a x)$

Assume a lognormal probability distribution with mean value $m_x = 6$ and variable standard deviation s_x ($a = 1$):

Error in x (%)	s_x	$f(m_x)$	$\langle y \rangle^a$	Ratio ^b
1	0.06	0.0024788	0.0024832	1.0018
2	0.12	0.0024788	0.0024966	1.0072
5	0.3	0.0024788	0.0025911	1.0453
10	0.6	0.0024788	0.0029380	1.1853
20	1.2	0.0024788	0.0044566	1.7979
50	3	0.0024788	0.018399	7.4225
100	6	0.0024788	0.071661	28.909

Assume a lognormal probability distribution with mean value $m_x = 6$ and variable parameter “a” ($s_x = 0.3$):

“a”	$f(m_x)$	$\langle y \rangle^a$	Ratio ^b
0.1	0.54881	0.54906	1.0005
0.2	0.30119	0.30174	1.0018
0.5	0.049787	0.050346	1.0112
1	0.0024788	0.0025911	1.0453
2	6.1442×10^{-6}	7.3178×10^{-6}	1.1910
5	9.3576×10^{-14}	2.6691×10^{-13}	2.8523
10	8.7565×10^{-27}	4.4776×10^{-25}	51.134

^a $\langle y \rangle = \int f(x) p(x) dx$ where $p(x)$ is the indicated lognormal distribution; values in tables are computed numerically using a spreadsheet program.

^b Ratio = $\langle y \rangle / f(m_x)$.

Table 10: The effects of error and error amplification for the simple non-linear function $y = f(x) = \exp(-a / x)$

Assume a lognormal probability distribution with mean value $m_x = 6$ and variable standard deviation s_x ($a = 1$):

Error in x (%)	s_x	$f(m_x)$	$\langle y \rangle^a$	Ratio ^b
1	0.06	0.84648	0.84647	0.99999
2	0.12	0.84648	0.84643	0.99994
5	0.3	0.84648	0.84616	0.99962
10	0.6	0.84648	0.84519	0.99848
20	1.2	0.84648	0.84136	0.99395
50	3	0.84648	0.81612	0.96413
100	6	0.84648	0.74538	0.88056

Assume a lognormal probability distribution with mean value $m_x = 6$ and variable parameter “a” ($s_x = 0.3$):

“a”	$f(m_x)$	$\langle y \rangle^a$	Ratio ^b
0.1	0.98347	0.98343	0.99996
0.2	0.96722	0.96714	0.99992
0.5	0.92004	0.91986	0.99980
1	0.84648	0.84616	0.99962
2	0.71653	0.71603	0.99930
5	0.43460	0.43407	0.99878
10	0.18888	0.18875	0.99931
20	0.035674	0.035871	1.0055
50	0.00024037	0.00025642	1.0668
100	5.7778×10^{-8}	7.7484×10^{-8}	1.3411

^a $\langle y \rangle = \int f(x) p(x) dx$ where $p(x)$ is the indicated lognormal distribution; values in tables are computed numerically using a spreadsheet program.

^b Ratio = $\langle y \rangle / f(m_x)$.

Figure Captions

Figure 1: Plots are shown of normal distributions $p(x)$ with mean value $m_x = 100$ and standard deviations $s_x = 1, 10, 20, 50, 100,$ and $150,$ respectively. These distributions are normalized so that $p(m_x = 100) = 1.$ It is obvious from the plots that there is a significant probability of encountering a negative value of x when $s_x \geq 50.$

Figure 2: The fraction of total integrated probability (given in percent) for a normal distribution that corresponds to negative values of x is plotted as a function of the distribution standard deviation (also expressed in percent).

Figure 3: Plots are shown of lognormal distributions $p(x)$ with mean value $m_x = 100$ and standard deviations $s_x = 1, 10, 20, 50, 100,$ and $150,$ respectively. These distributions are normalized so that $p(x_0) = 1,$ where $x_0 = \exp(\nu - \sigma^2)$ is the mode of the distribution. It is obvious from these plots that the lognormal distribution is strongly asymmetric for large values of $s_x.$

Figure 4: The shapes of normal and lognormal distributions $p(x)$ with equivalent mean values m_x and standard deviations s_x are compared. Four examples are considered: $s_x = 20, 50, 100,$ and $150.$ These functions are normalized so that the integrals $\int p(x)dx$ are equal for both curves shown in each frame. Evidently, the shapes of the normal and lognormal distributions are not easily distinguished when $s_x \approx 20$ (error $\approx 20\%$), so no plots are shown that involve errors smaller than this value.

Figure 5: A lognormal function with mean value $m_x = 10$ and standard deviation $s_x = 5$ (50% error) is plotted as a smooth curve. The empirical replication of this distribution generated by Monte Carlo simulation – with $N = 100000$ sampling histories and 30 intervals of equal increment in the variable x – is also exhibited. These two distributions are normalized identically in order to provide a meaningful comparison.

Figure 6: The probability density function (PDF) for natural logarithm of residual radioactivity – as discussed in the example presented in Section 9 – is shown using both linear and semi-log scales. The discrete points were generated by Monte Carlo simulation while the smooth curve is an analytical normal distribution with mean value and standard deviation also generated by the same Monte Carlo analysis.

Figure 7: The probability density function (PDF) for natural logarithm of 662-keV ^{137}Cs gamma-ray intensity transmitted through lead shielding – as discussed in the example presented in Section 10 – is shown using both linear and semi-log scales. The discrete points were generated by Monte Carlo simulation while the smooth curve is an analytical normal distribution with mean value and standard deviation also generated by the same Monte Carlo analysis.

Figure 8: Relative contributions to the stellar reaction rate from the first five unbound resonances in the $^{31}\text{P}(p,\gamma)^{32}\text{S}$ reaction are shown in bar-graph form for nine

different stellar temperatures T_9 . The resonance data used in generating these plots are obtained from Table 3 and the detailed analysis is described in Section 11. Although they are unlabelled, the vertical scales in these plots are linear and they exhibit the relative contributions from these resonances in proper proportion. The individual resonances are numbered in order of ascending incident proton energy, with “1” denoting the lowest-energy resonance and “5” denoting the highest-energy resonance of this group.

Figure 9: Mean values and standard deviations of reaction rates for the $^{31}\text{P}(p,\gamma)^{32}\text{S}$ reaction obtained by deterministic calculations and Monte Carlo simulation using Eq. (40) are compared by plotting ratios as a function of stellar temperature T_9 . In this figure $\langle R \rangle$ denotes the average value of a lognormal probability distribution for reaction rate that was obtained by transformation from the parameters of its equivalent, empirically determined normal distribution for the natural logarithm of reaction rate $\ln R$. R_{det} is the corresponding quantity obtained by deterministic calculations. Error $\langle R \rangle$ and Error R_{det} denote corresponding standard deviations in these parameters. It is seen that noticeable differences arise between the results generated by these two methods for $T_9 < 0.1$ GK.

Figure 10: Probability distributions for natural logarithms of reaction rates are shown for stellar temperatures $T_9 = 0.011$ and 0.1 GK using both linear and semi-logarithmic scales (Section 11). The individual points that are shown in these plots were generated by Monte Carlo simulation; the smooth curves are equivalent normal distributions with mean values and standard deviations that were also produced by the Monte Carlo analyses.

Figure 11: Quality-of-fit factors and quality-of-agreement indicators are plotted based on results given in Tables 7 and 8 (Section 11). Natural Logarithm of Reaction Rate: Quality of Fit = $[\langle \ln R \rangle_{\text{data}} - \langle \ln R \rangle_{\text{fit}}] / (\text{Error } \ln R)_{\text{data}}$. Error in Natural Logarithm of Reaction Rate: Quality of Fit = $\{(\text{Error } \ln R)_{\text{data}} - (\text{Error } \ln R)_{\text{fit}}\} / [0.1 \times \langle \ln R \rangle_{\text{data}}]$. Reaction Rate: Quality of Agreement = $[\langle R \rangle_{\text{data}} - \langle R \rangle_{\text{fit}}] / (\text{Error } R)_{\text{data}}$.

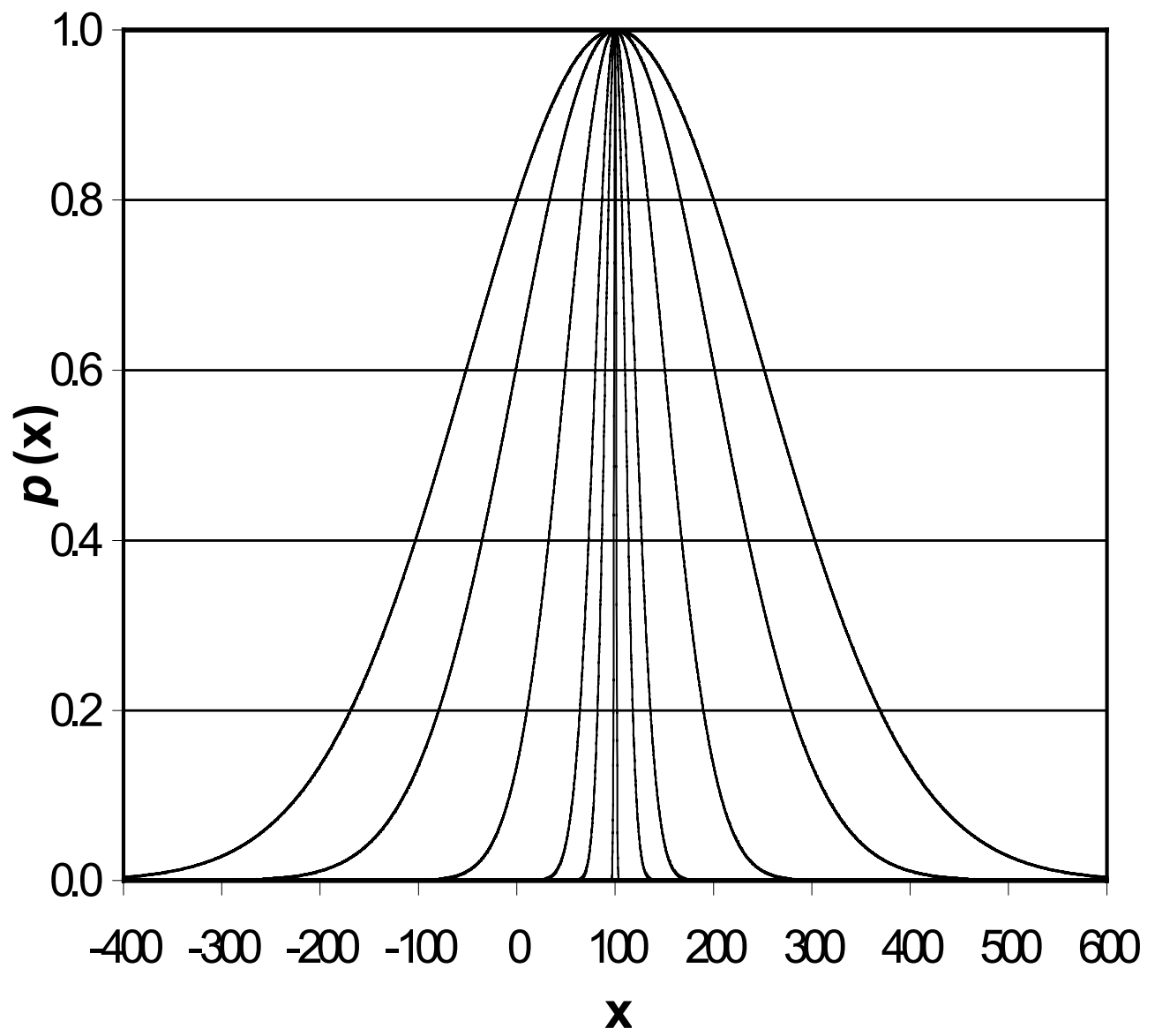


Figure 1

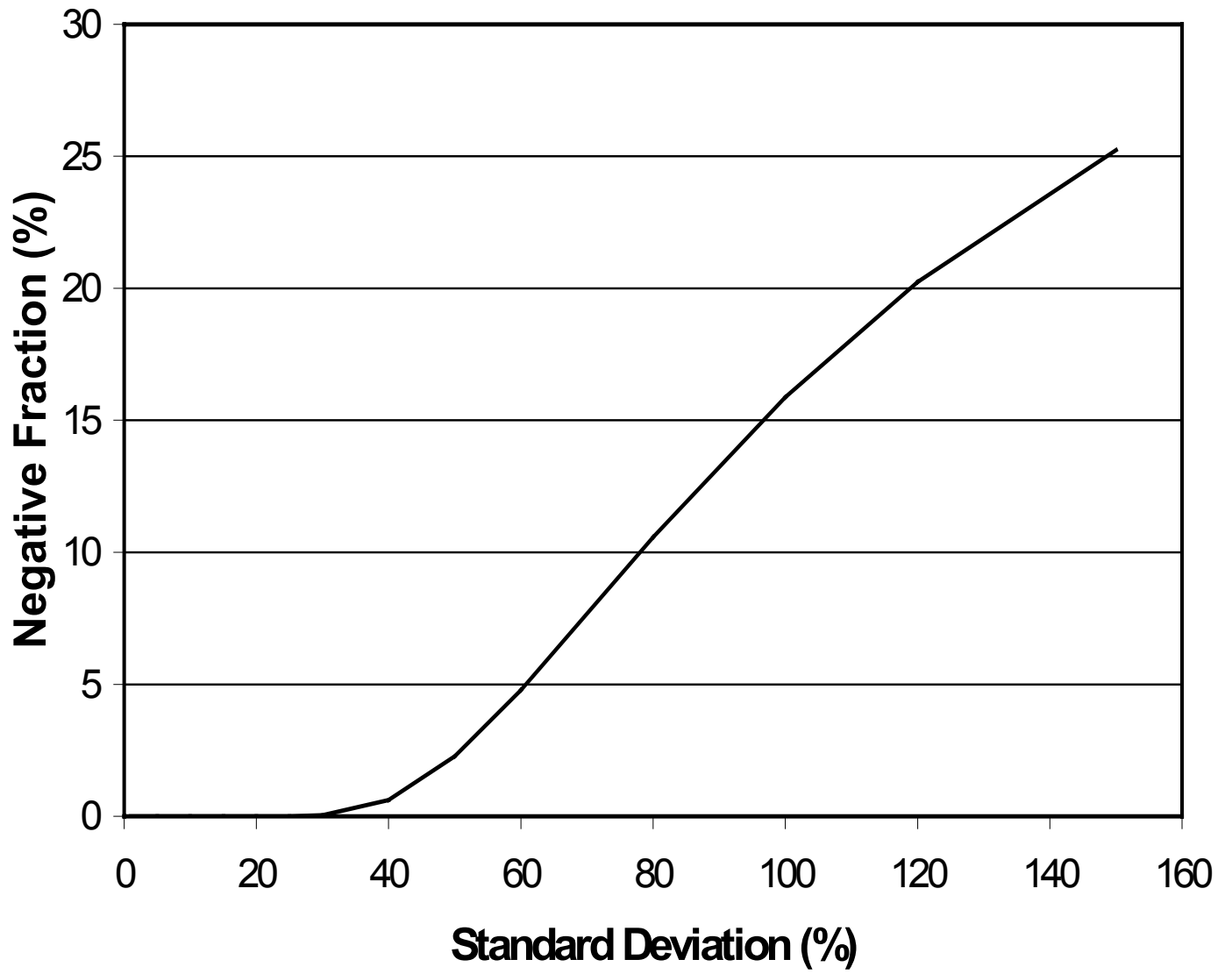


Figure 2

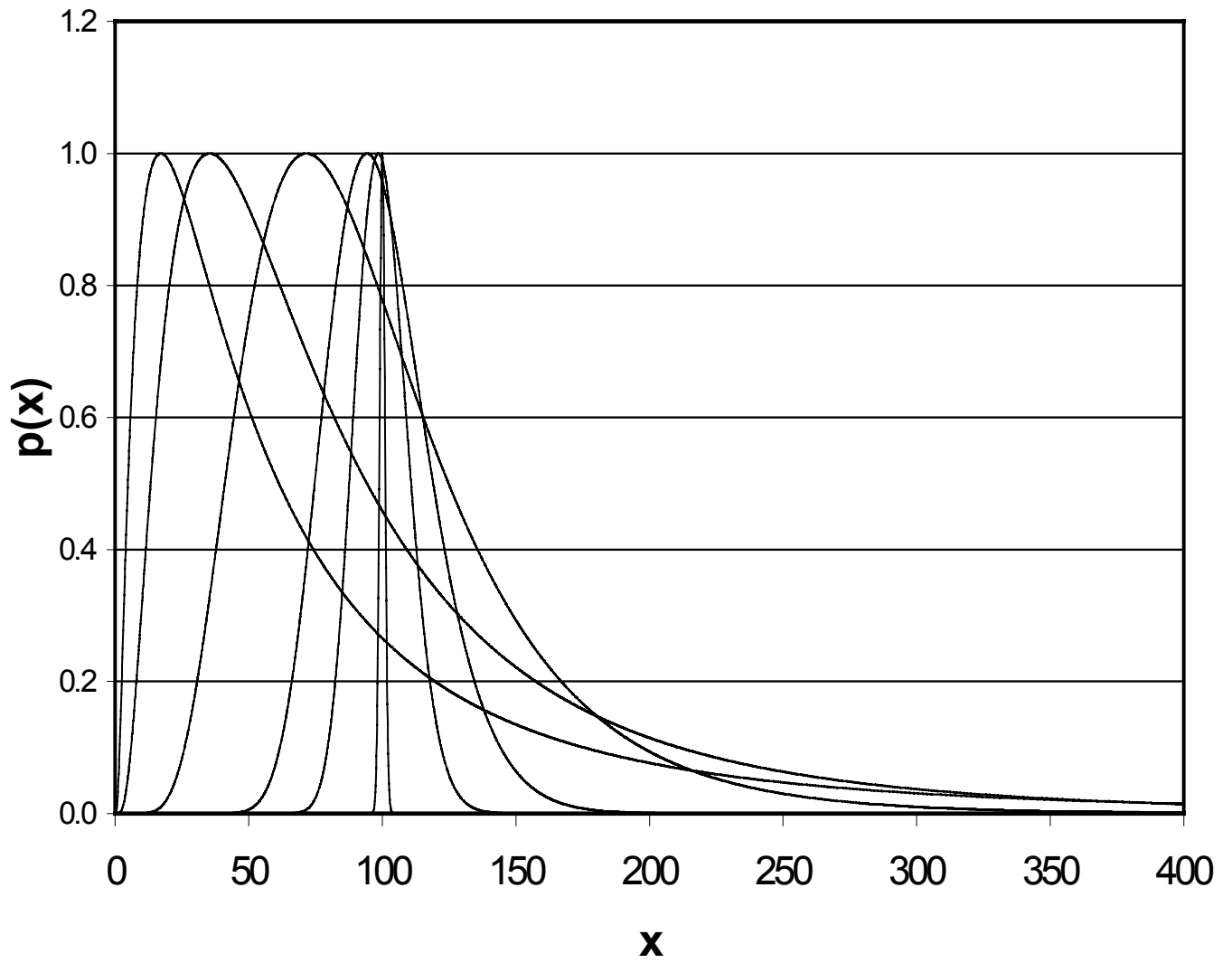


Figure 3

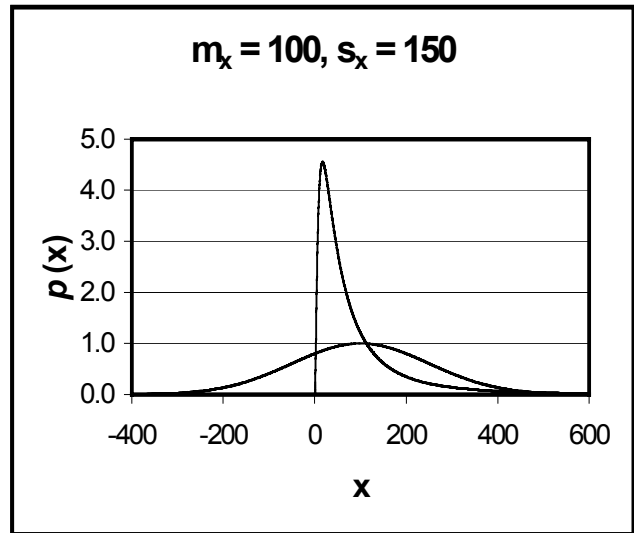
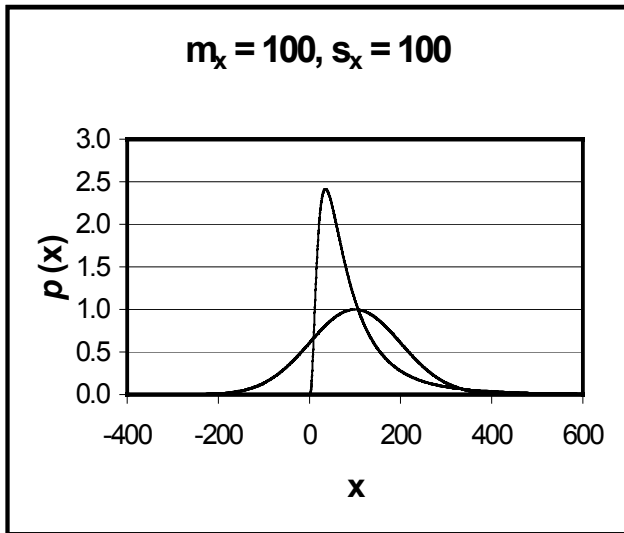
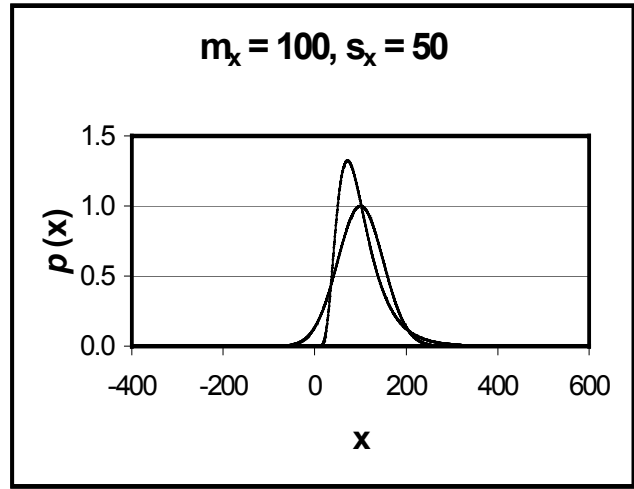
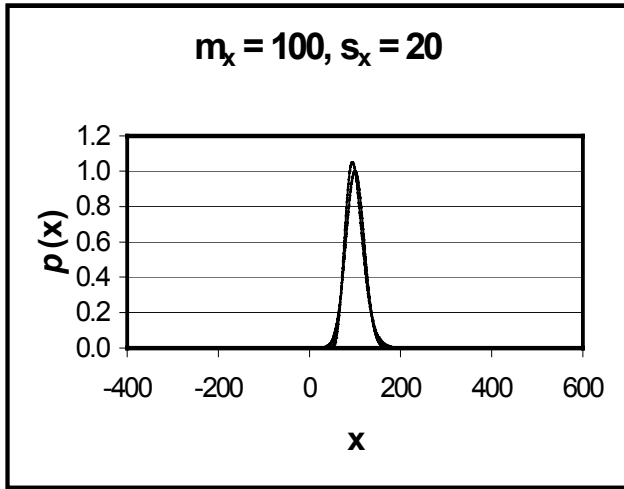


Figure 4

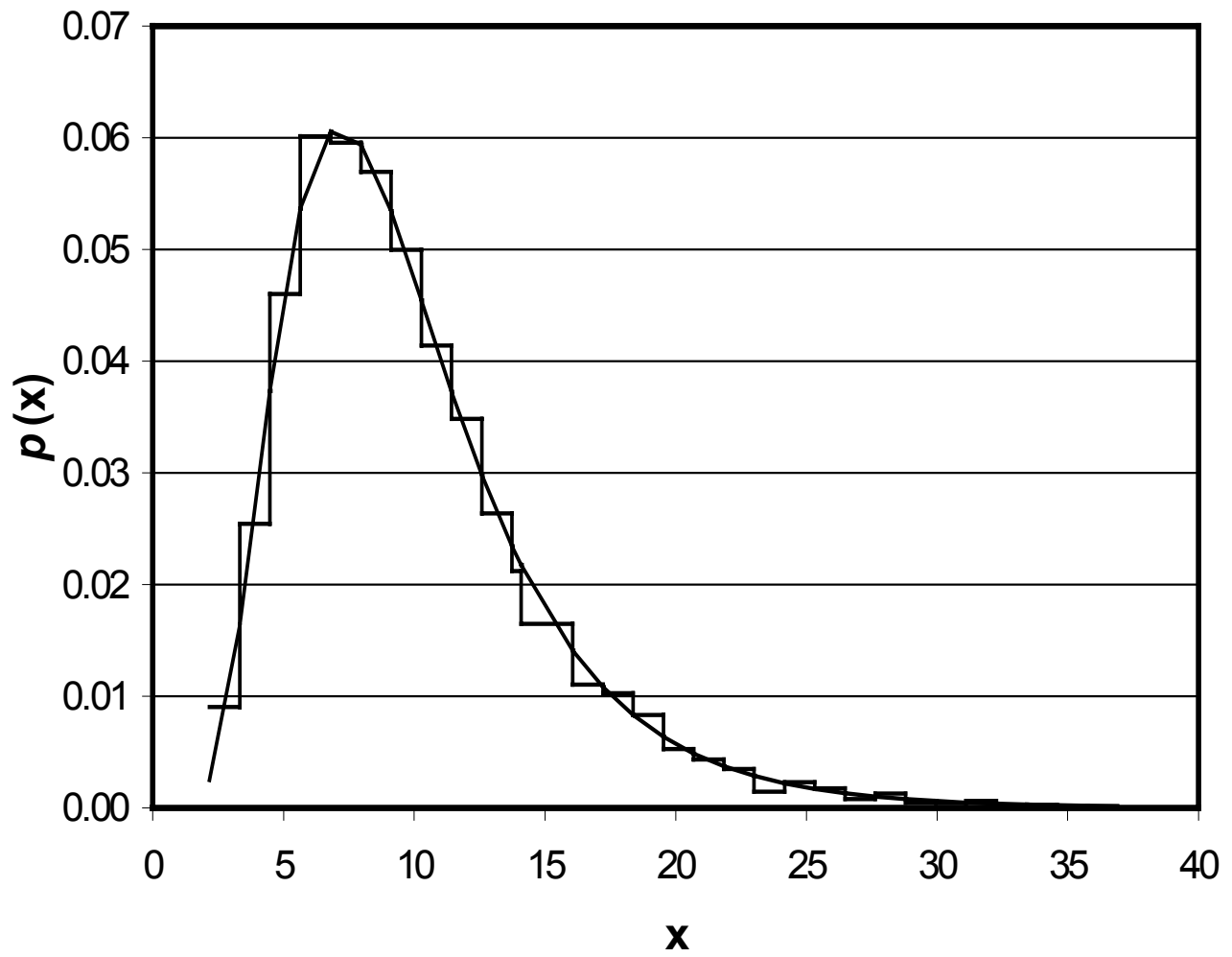


Figure 5

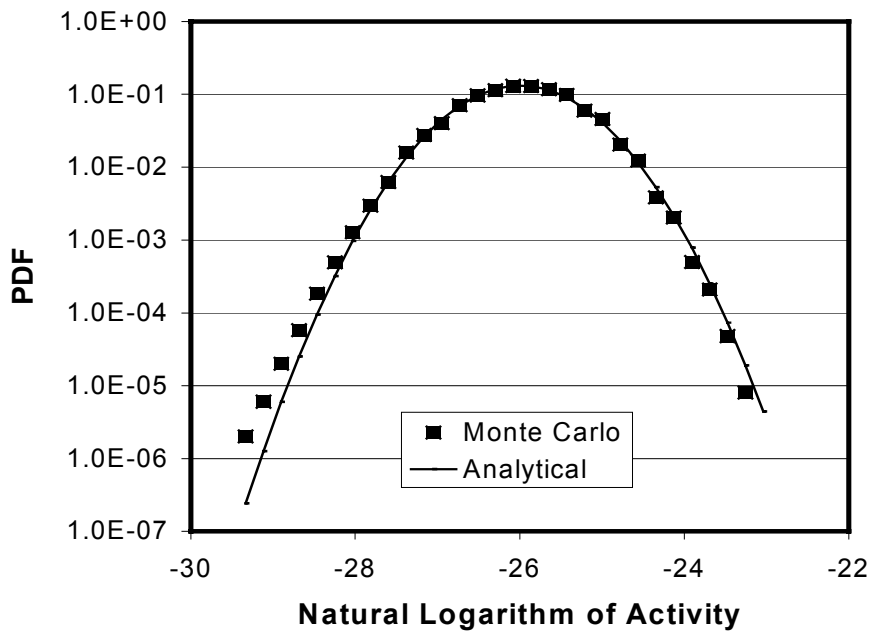
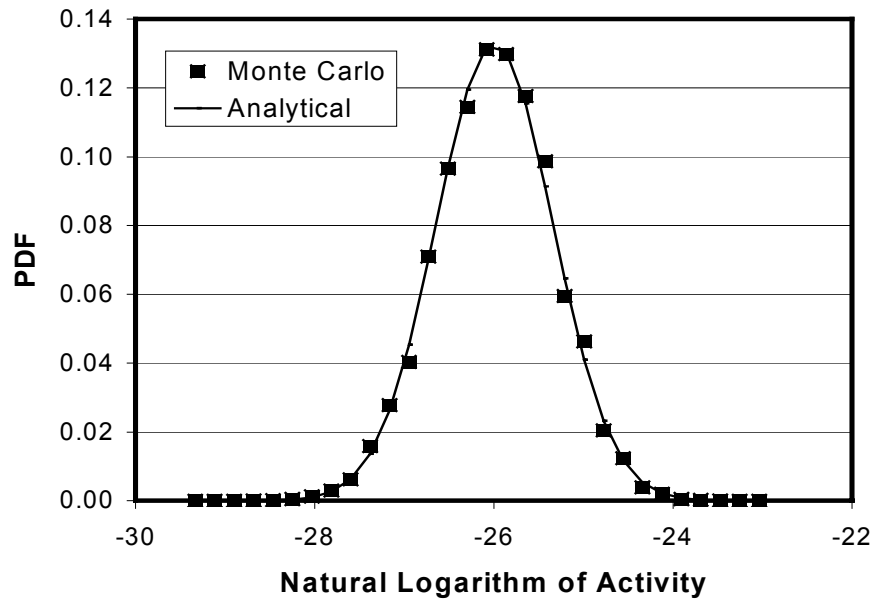


Figure 6

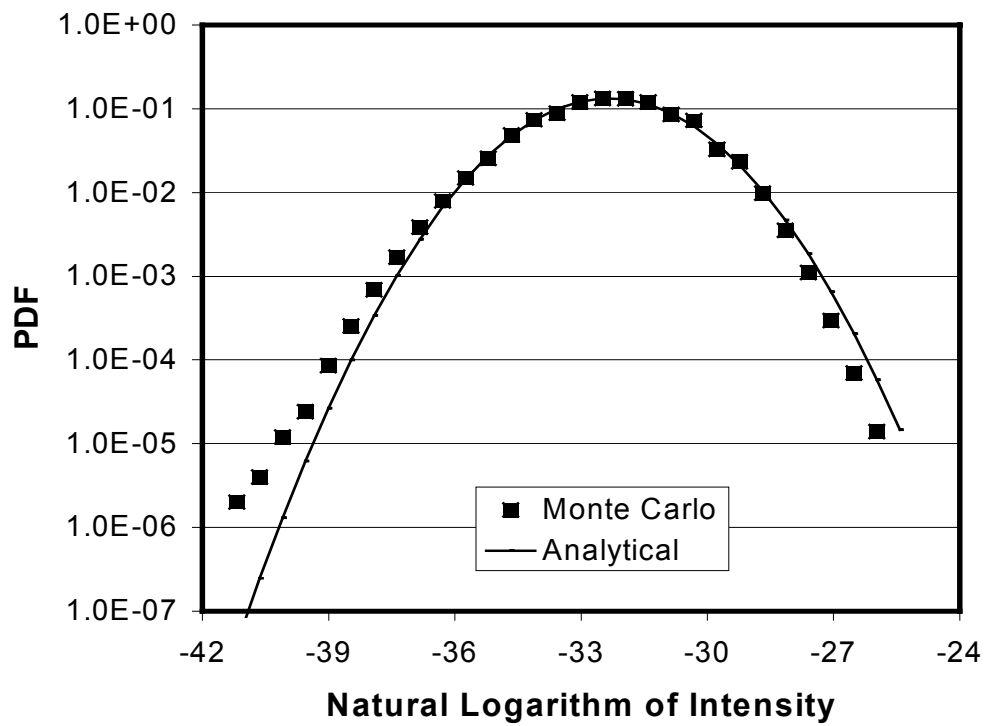
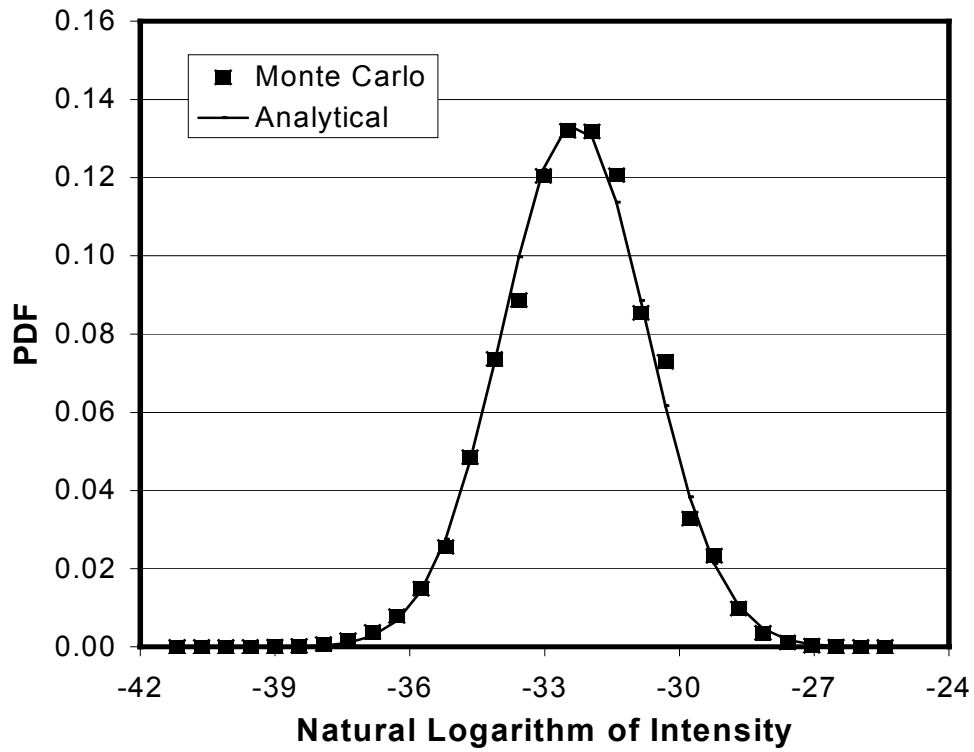


Figure 7

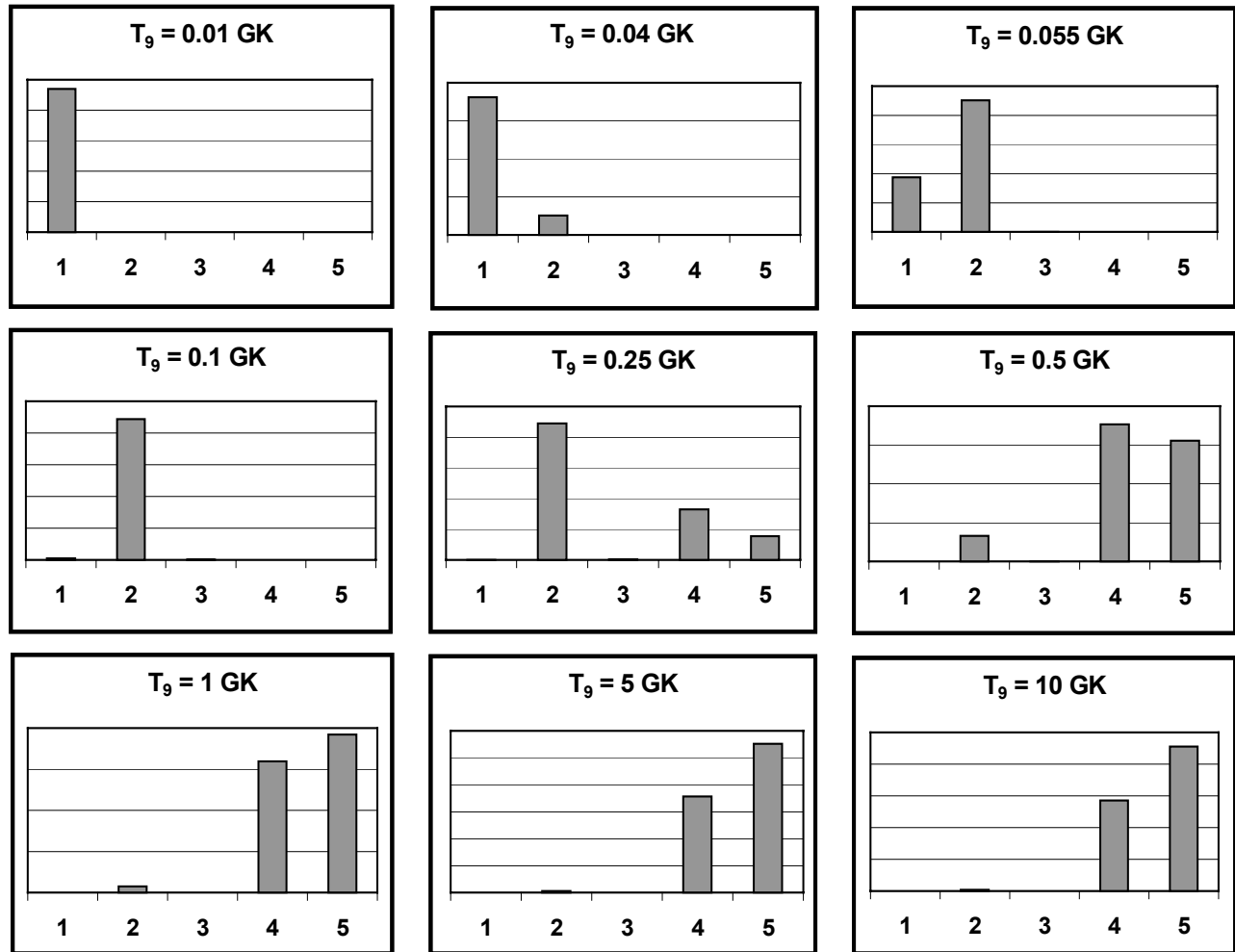


Figure 8

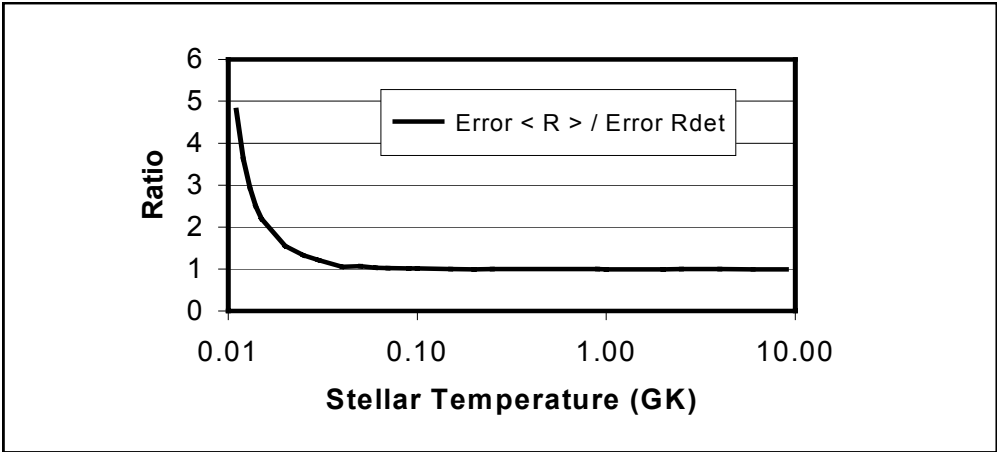
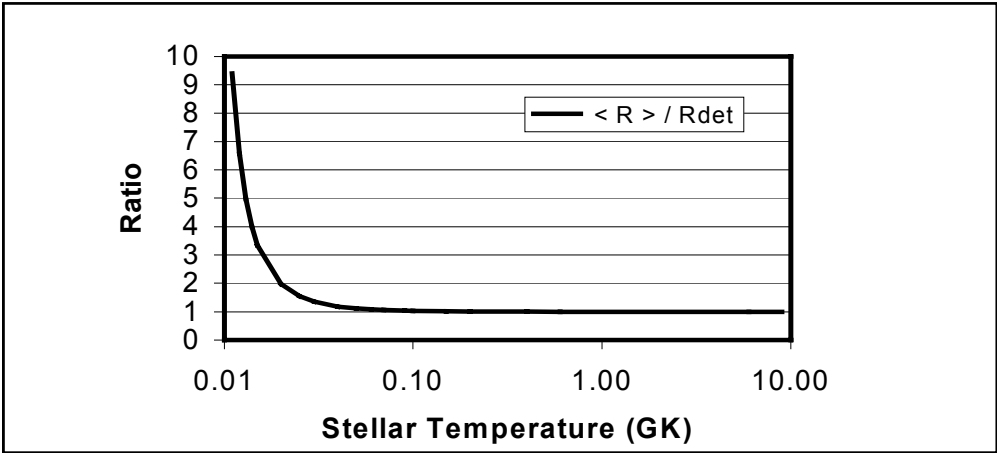


Figure 9

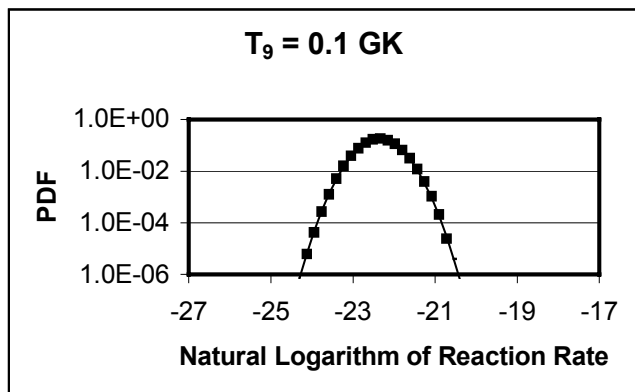
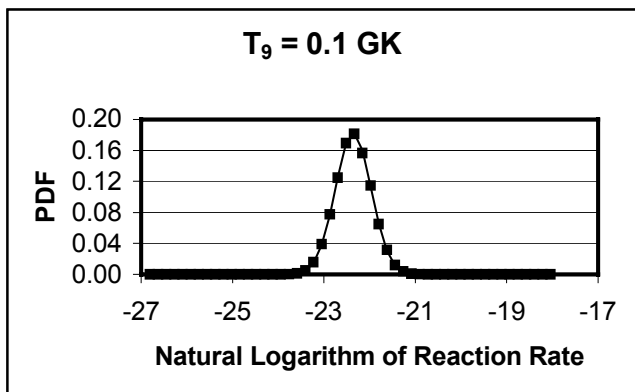
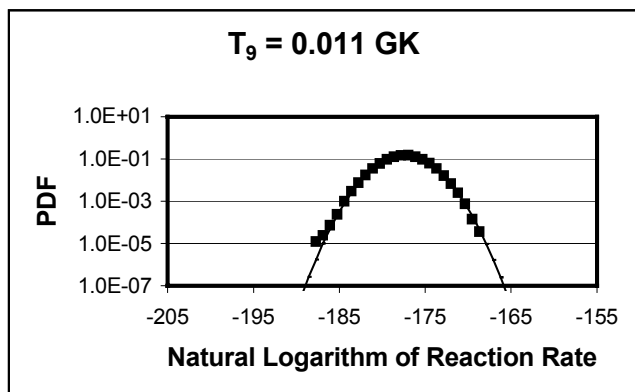
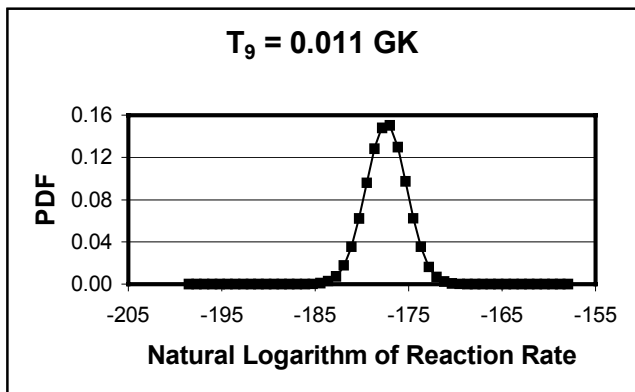


Figure 10

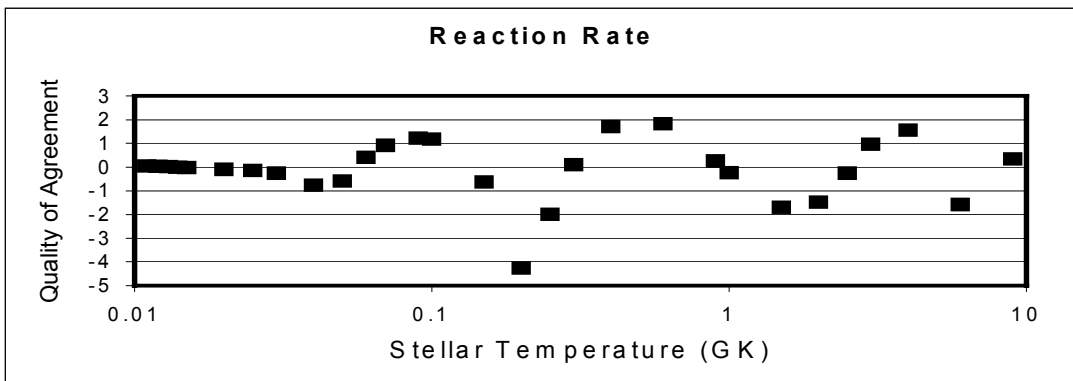
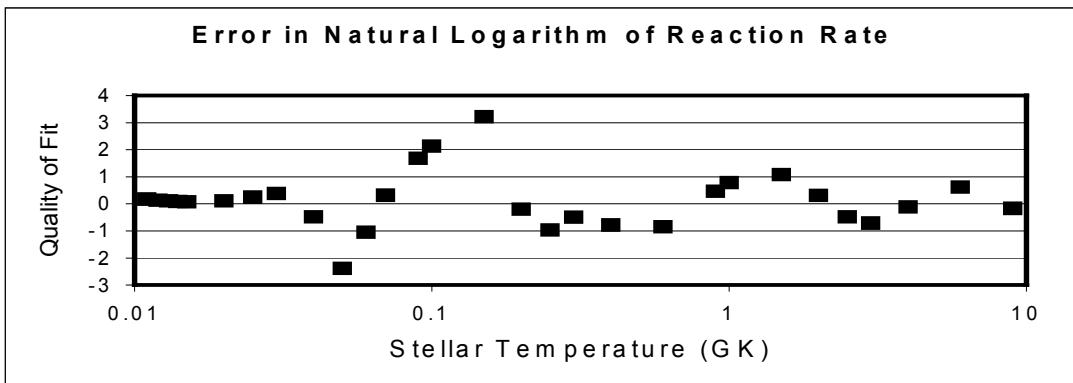
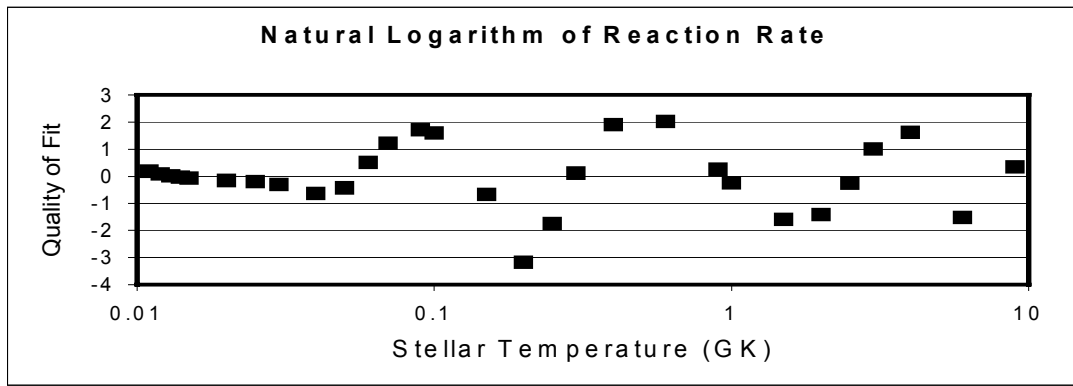


Figure 11

Blank Page